CLEARINGHOUSE FOR FEDERAL SCIENTIFIC AND TECHNICAL INFORMATION CFSTI
DOCUMENT MANAGEMENT BRANCH 410.11

LIMITATIONS IN REPRODUCTION QUALITY

ACCESSION # 603947

- [x] 1. WE REGRET THAT LEGIBILITY OF THIS DOCUMENT IS IN PART UNSATISFACTORY. REPRODUCTION HAS BEEN MADE FROM BEST AVAILABLE COPY.
- [x] 2. A PORTION OF THE ORIGINAL DOCUMENT CONTAINS FINE DETAIL WHICH MAY MAKE READING OF PHOTOCOPY DIFFICULT.
- [ ] 3. THE ORIGINAL DOCUMENT CONTAINS COLOR, BUT DISTRIBUTION COPIES ARE AVAILABLE IN BLACK-AND-WHITE REPRODUCTION ONLY.
- [ ] 4. THE INITIAL DISTRIBUTION COPIES CONTAIN COLOR WHICH WILL BE SHOWN IN BLACK-AND-WHITE WHEN IT IS NECESSARY TO REPRINT.
- [ ] 5. LIMITED SUPPLY ON HAND: WHEN EXHAUSTED, DOCUMENT WILL BE AVAILABLE IN MICROFICHE ONLY.
- [ ] 6. LIMITED SUPPLY ON HAND: WHEN EXHAUSTED DOCUMENT WILL NOT BE AVAILABLE.
- [ ] 7. DOCUMENT IS AVAILABLE IN MICROFICHE ONLY.
- [ ] 8. DOCUMENT AVAILABLE ON LOAN FROM CFSTI (TT DOCUMENTS ONLY).
- [ ] 9.

PROCESSOR: PM

TSL-107-10/64

FTD-TT- 64-497

TRANSLATION

THE PROBLEM OF DETERMINING THE OPTIMUM CRITICAL OPERATING PARAMETERS FOR A NONISOBARIC MOTOR WITH DIVERGENT NOZZLE

By

R. Staniszewski

FOREIGN TECHNOLOGY DIVISION

AIR FORCE SYSTEMS COMMAND

WRIGHT-PATTERSON AIR FORCE BASE

OHIO

EDITED TRANSLATION

THE PROBLEM OF DETERMINING THE OPTIMUM CRITICAL OPERATING PARAMETERS FOR A NONISOBARIC MOTOR WITH DIVERGENT NOZZLE

BY: R. Staniszewski

English Pages: 53

SOURCE: Archiwum Budowy Maszyn (Polish), Vol. 10, Nr. 2, 1963, pp 103-140

P/0032-063-010-002

THIS TRANSLATION IS A RENDITION OF THE ORIGINAL FOREIGN TEXT WITHOUT ANY ANALYTICAL OR EDITORIAL COMMENT. STATEMENTS OR THEORIES ADVOCATED OR IMPLIED ARE THOSE OF THE SOURCE AND DO NOT NECESSARILY REFLECT THE POSITION OR OPINION OF THE FOREIGN TECHNOLOGY DIVISION.	PREPARED BY: TRANSLATION DIVISION FOREIGN TECHNOLOGY DIVISION WP-AFB, OHIO.

THE PROBLEM OF DETERMINING THE OPTIMUM CRITICAL OPERATING PARAMETERS FOR A NONISOBARIC MOTOR WITH DIVERGENT NOZZLE

Robert Staniszewski

Warsaw

The author solves the problem of nonsteady state operation of a liquid rocket motor, using the dynamical differential equations of turbulent flow. He uses the solutions to determine the optimum and critical parameters, together with the stability limits, on the basis of a nonisobaric motor model. The determination of these parameters makes it possible to correct the design method used for rocket motors.

1. INTRODUCTION

Existing design methods for liquid rocket motors are based on steady-state hydro-, thermo-, and gasdynamical equations, and do not allow for nonsteady states. Theoretical and experimental studies have shown that the phenomena occurring during the various stages of engine operation frequently are far from steady. Considerable parameter variations, most frequently of pulsating nature, and taking the form of pressure and temperature oscillations, occur during startup. Disturbances reaching the fuel-supply system may pass through the various fuel lines into the combustion chamber, upsetting combustion stability. In some cases, these disturbances may be sufficiently damped, so that they will have only a negligible effect on the stability of the engine operating parameters. In other cases, however, they may be intensified as they travel, so that they reach the combustion chamber as strong disturbances. This may throw the engine into an unstable operating mode. The nonsteady states mentioned distort the propulsion characteristics and act as a source of vibration for on-board installations and the aircraft structure. Under certain conditions, they may damage the engine. The aim of this work was therefore to investigate the nonstationary phenomena occurring in a rocket motor. All nonsteady states were reduced to four groups: unsteady fuel-system operation, engine startup, unsteady combustion, and unstable operation. Results for these individual groups of disturbances were used to work out corrections for the steady-state design method used for liquid rocket motors.

PRINCIPAL NOTATION

ρ = density,

T = temperature,

τ, t = time,

ζ = line loss coefficient,

p = pressure,

L_{ks} = length of combustion chamber,

W = flow velocity,

V_{ks} = volume of combustion chamber,

F = cross-sectional area,

l = length,

R_0, R = gas constant, resistance coefficient, radius,

t_0 = time mixture is in combustion chamber,

ω = pulsation, characteristic volume,

f = area of transverse injector cross section,

Δp_g = pressure drop across injector nozzle,

G, q = flow rate (weight, mass),

μ = injection-loss coefficient,

γ = specific gravity,

t' = ignition lag time,

λ = combustion-chamber loss coefficient, and z = variable chamber length.

SUBSCRIPTS

1 = parameters ahead of reduction valve,

2 = parameters after reduction valve,

3 = parameters after tank,

4 = parameters after cooling chamber,

5 = injection parameters,

0 = parameters in combustion chamber,

kr = critical parameters,

m = number of injectors per component,

m' = total number of injectors,

opt = optimum parameters,

nz = quantity referring to nonisobaric engine,

iz = quantity referring to isobaric engine,

u = parameters in steady range, and

z = fuel-system parameters.

2. ASSUMPTIONS

Solution of the problem of nonsteady states was reduced to examination of the four characteristic states which essentially cover the most severe engine-performance conditions. Despite the differences among the disturbances with respect to their nature, point of action, or effects, all types of disturbances may be reduced to the types outlined here. When disturbances resulting from a change in flight characteristics or induced by airfoil design upset parameter stability in the turbopump pressure-accumulator system or the combustible or oxidant installation, we must deal with transients in the propellant-supply system. These disturbances may be so weak that they will be damped even before reaching the injector nozzle. On the contrary, however, they may become so strong (being intensified as they travel) that they reach the

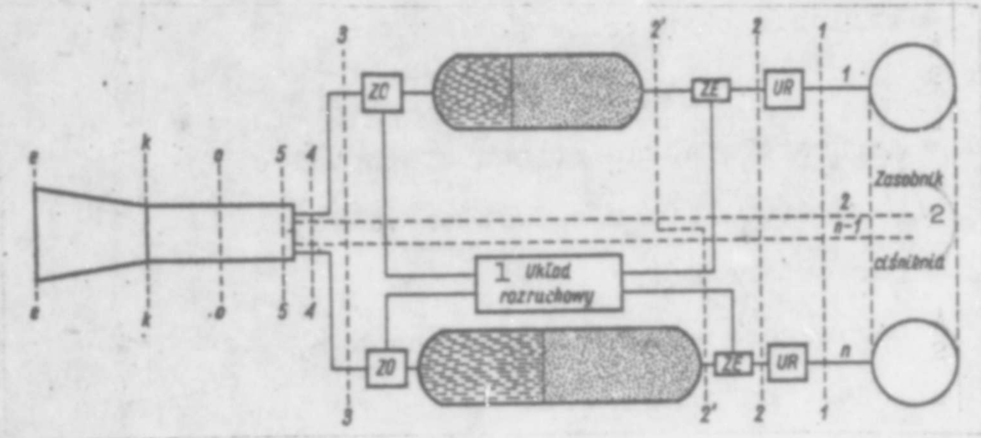

Fig. 1. 1) Starting system; 2) pressure accumulator.

chamber, upset combustion-process stability, and cause a change in pressure. The combustion process may also be disturbed by improper arrangement of the injectors. In both the first and second cases we must deal with unsteady combustion. Presence of such transients in the propellant-supply system, as well as unsteady combustion, is marked by changes in parameters within certain definite ranges. If, however, the disturbance is so strong as to produce a continuous increase in parameters with time (for example, during startup) as, for example, in the chamber pressure, we are concerned with unstable operation. Engine startup and the three types of instability mentioned above will be the subject of a detailed examination.

The following were assumed in the consideration of the problem:

1. A nonisobaric engine (Fig. 1).

2. The average value of engine thrust, specific thrust, and overall flow rate are taken constant between the startup period and engine cut-out; hence

$$\bar{K} = \frac{\int_{-T/2}^{T/2} K_{(\tau)} T d\tau}{\int_{-T/2}^{T/2} T d\tau}, \qquad (1)$$

$$\bar{k}_j = \frac{\int_{-T/2}^{T/2} k_{j(\tau)} T d\tau}{\int_{-T/2}^{T/2} T d\tau}. \qquad (2)$$

$$\bar{G} = \frac{\int_{-T/2}^{T/2} G_{(\tau)} T d\tau}{\int_{-T/2}^{T/2} T d\tau}. \qquad (3)$$

3. The problem of parameter variation during disturbances is reduced to a change in pressure with time

$$F[p_{(\tau)}, W_{(\tau)}, \rho_{(\tau)}, T_{(\tau)}] \to p_{(\tau)}. \qquad (4)$$

4. It is assumed that the propellant is made up of n components, each having a separate line.

5. On the first assumption, we may use small-perturbation theory for the nonlinear relationship $G = \varphi(p)$, and reduce this function to a linear relationship. This assumption is in fact important when we consider transients in the propellant-supply system and unsteady combustion.

6. Spatially averaged parameters will be considered, hence:

$$\bar{p} = \frac{\int\limits_{\omega} \rho p d\omega}{\int\limits_{\omega} \rho d\omega}, \quad T = \frac{\int\limits_{\omega} \rho T d\tau}{\int\limits_{\omega} \rho d\tau}, \quad \bar{W} = \frac{\int\limits_{\omega} \rho W d\tau}{\int\limits_{\omega} \rho d\tau}. \qquad (5)$$

As we know, most rocket motors are designed for constant thrust; hence the first assumption is fully justified. The choice of pressure variation was dictated by the possibility of eventually confirming the theoretical studies by means of experimental results obtained from pressure measurements with the aid of suitable data. Generalization of the problem required the adoption of the third condition. In practice, it frequently happens that the propellant is made up of three or even four components. Estimation of errors shows that the assumption of a linear relationship for the functions $G = \varphi(p)$ and $W = \psi(p)$ yields sufficient accuracy. If this assumption were carried over to a variable-thrust engine, especially where K varies over a wide range, the total pattern of the phenomenon taking place might in fact be obscured. Calculations show that for a pressure variation of about 20% with respect to the calculated value, the error resulting from the assumption of linear variation amounts to about 1.5%. For a case of thrust with constant K, this is sufficient.

This study presents one method for solving the problem of the nonsteady states in a liquid rocket engine, together with an examination of the results yielded by the computational method for this type of propulsion. In no case do we pretend to present an exhaustive and complete solution of this problem, especially since many scientists (Crocco, Bodner, Tsien, Tischler, Belman, Gore, Lee, Ross Gunder, Summerfield, Reichel, Grey, Harrje, and others) are working on it.

Experimental findings indicate that disturbances propagate along the direction of flow of the propellant components and the gases in the combustion chamber. In some cases, however, disturbances will move in the opposite direction. Most cases of this sort were observed in the injector system. During strong disturbances, variations in pressure inside the combustion chamber were found to have a distinct effect on the pressure head of the injector. Since this problem must be dealt with before certain nonsteady states are examined, it will be useful if we first consider unsteady combustion. The problems of startup, transients in the fuel system, and unstable operation will then be taken up in turn.

3. THE PROBLEM OF UNSTEADY COMBUSTION

Let us consider the problem of unsteady combustion in the chamber of a nonisobaric rocket engine using an n-component propellant. The problem will be solved for the propulsion case with constant average fundamental parameters. We shall confine ourselves to an engine with linear characteristic geometry for the chamber and nozzle; hence:

for the chamber

$$F_{\Phi(z)} = \mathrm{const}, \tag{6}$$

for the nozzle

$$R_{(z)} = R_k + z\frac{dr}{dz}, \tag{7}$$

where dr/dz = const.

In accordance with Crocco's fundamental thesis, the cause of unstable combustion is the existence of a certain time interval between the instant the mixture is introduced into the combustion chamber and the moment of ignition. Crocco divides this time, otherwise known as the ignition lag, into two components: a constant portion t" characteristic of the given propellant, and a variable portion t"', which depends on the operating conditions. The existence of an ignition lag that can vary in either time or space results in inhomogeneity of the gas mixture at the flame front. The resulting nonuniform release of heat leads to temperatures that differ both at various points in space or at different times at the same point. Since energy levels tend to seek equilibrium, in such case there will be a change in the temperature and pressure. It would thus appear that there has been a change in the mixture composition due to an over- or under-supply of one of the components, and hence a change in the over-all density at the points of inhomogeneity. Remembering that the density, in general, is also related to velocity, position, and time, we can write

$$\rho = F[C_{(u,v,w)}, P_{(x,y,z)}, T, p, \tau]. \tag{8}$$

Thus we can reduce the problem of studying unsteady combustion to that of studying mixture composition by finding the change in density:

$$d\rho = \frac{\partial\rho}{\partial v}\frac{\partial v}{\partial\tau}d\tau + \frac{\partial\rho}{\partial u}\frac{\partial u}{\partial\tau}d\tau + \frac{\partial\rho}{\partial w}\frac{\partial w}{\partial\tau}d\tau + \frac{\partial\rho}{\partial x}dx + \frac{\partial\rho}{\partial y}dy + \frac{\partial\rho}{\partial z}dz + \frac{\partial\rho}{\partial p}\frac{\partial p}{\partial\tau}d\tau + \frac{\partial\rho}{\partial T}\frac{\partial T}{\partial\tau}d\tau, \quad (9)$$

going from the density of the liquid components to the density of the gas. Thus in unsteady combustion, ρ will be a complex function varying in space and time. Each local change in mixture composition, even in the atomization zone, will immediately be transmitted to the combustion zone, resulting in changes in the thermal quantities. If at an arbitrary point in the atomization zone, the mixture composition changes with respect to the optimum composition, the change will immediately be propagated to the combustion zone, resulting in local excess heat release. The increased heat produces a rise in the temperature and pressure and, owing to the existence of the surrounding lower energy level, this point will automatically become the source of a disturbance that causes a thermal wave to propagate. The waves formed are characterized by temperature and pressure pulsations; they are continuous in nature for small disturbances, but may become shock waves with larger disturbances. Thus the factor responsible for unsteady combustion is a local change in mixture composition, which produces a local difference in density. For two arbitrary points A and B in the flame-front space, the expression

$$\rho_{(A)} - \rho_{(B)} = \int_A^B \left[\frac{\partial\rho}{\partial v}\frac{\partial v}{\partial\tau}d\tau + \frac{\partial\rho}{\partial u}\frac{\partial u}{\partial\tau}d\tau + \frac{\partial\rho}{\partial w}\frac{\partial w}{\partial\tau}d\tau + \frac{\partial\rho}{\partial p}\frac{\partial p}{\partial\tau}d\tau + \frac{\partial\rho}{\partial T}\frac{\partial T}{\partial\tau}d\tau\right] \quad (10)$$

does not equal zero for unsteady combustion. Analyzing the combustion process, we conclude that a change in mixture composition can be either stationary or nonstationary. The first case results from incorrect injector arrangement, and we shall not consider this problem here.

Let us examine the problem of nonstationary variation in mixture composition. We have established that such a variation will be accompanied by a change in the density of the medium. Allowing for the different densities of the fuel and oxidizer groups, we conclude that a deviation in the gas density at the flame front from the calculated value can only be produced by a change in the flow-rate of one or more of the components. We thus reduce the problem of studying unsteady combustion to one of studying mixture composition, in terms of the variations in the concentrations of the propellant components. Here we note that a local disturbance at the flame front will not only cause an unsteady outflow, but also a displacement in the direction opposite to that in which the gas is flowing. Small disturbances may be damped as they travel, so that they do not reach the injector, but stronger disturbances may again produce a change in the flow-rate of some of the components. We shall refer to the first type of unsteady combustion as space-time unsteady combustion and the second type as space-time-secondary unsteady combustion.

We shall now derive the mathematical equations for space-time unsteady combustion. If disturbances in the chamber are produced by variations in the component flow rates, the change in mass at the flame front will be proportional to the change in the difference between the mass flow rates ahead of the injector and in the combustion chamber. We therefore have

$$\frac{d\overline{M}_{(\tau)}}{d\tau} = \sum_{1}^{N} q_{i(\tau-r)} - q_0, \qquad (11)$$

where $\overline{M}_{(\tau)}$ is the total mass of the mixture in the combustion chamber, where the mixture is composed of N phases.

Referring the chamber disturbances to changes in pressure and substituting the known functions

$$\frac{d\overline{M}_{(\tau)}}{d\tau} = \frac{V_{ks}}{gR_0 T_0} \frac{dp_{0(\tau)}}{d\tau}, \qquad (12)$$

$$q_0 = \frac{F_0 W_0}{g R_0 T_0} p_0, \tag{13}$$

where V_{ks} is the mixture volume in the chamber, and is made up of the volumes of the N phases, we obtain Eq. (11) in the form

$$\frac{V_{ks}}{g R_0 T_0} \frac{d p_{0(\tau)}}{d\tau} + \frac{F_0 W_0}{g R_0 T_0} p_{0(\tau)} = \sum_1^n q_{i(\tau-\tau_i)}. \tag{14}$$

The mass flow-rate at the injector can be represented with the aid of the following formulas:

$$\begin{aligned} q_{1(\tau-\tau_1)} &= \sqrt{\frac{2\gamma_1}{g}} \sqrt{\Delta p_{1(\tau-\tau_1)}} \sum_1^m f_i \mu_i, \\ q_{2(\tau-\tau_2)} &= \sqrt{\frac{2\gamma_2}{g}} \sqrt{\Delta p_{2(\tau-\tau_2)}} \sum_1^m f_i \mu_i, \\ &\cdots\cdots\cdots\cdots\cdots\cdots \\ q_{n(\tau-\tau_n)} &= \sqrt{\frac{2\gamma_n}{g}} \sqrt{\Delta p_{n(\tau-\tau_n)}} \sum_1^m f_i \mu_i \end{aligned} \tag{15}$$

where $\sum_1^m f_i \mu_i$ is the sum of the areas of the injector cross sections for the n components.

Since for our investigation Condition (1), (2) and (3) hold, so that the mass flow rates vary over a small range, the nonlinear relationship between the $q_{(\tau)}$ and Δp can be reduced to a linear variation. In accordance with the Taylor formula, we have

$$q = q_0 + \Delta q = q_0 + \frac{\partial q_0}{\partial \Delta p} \Delta\Delta p + \ldots + \frac{\partial^n q_0}{\partial \Delta p^n} \frac{(\Delta\Delta p)^n}{n!}, \tag{16}$$

and, after discarding nonlinear terms,

$$q_0 + \Delta q = q_0 + \frac{\partial q_0}{\partial \Delta p} \Delta\Delta p. \tag{17}$$

the derivative $\partial q_0 / \partial \Delta p$ will then take on a constant value and it can be represented by the tangent of the slope of the function

$$\frac{\partial q_0}{\partial \Delta p} = \frac{\sqrt{\frac{2\gamma}{g}}}{2\sqrt{\Delta p_m}} \sum_1^m f_i \mu_i = \operatorname{tg} \bar{\alpha}. \tag{18}$$

Using Eq. (14) in conjunction with Functions (15) and (16), we obtain

$$\frac{V_{ks}}{gR_0T_0}\frac{dp_{0(\tau)}}{d\tau}+\frac{F_0W_0}{gR_0T_0}p_{0(\tau)}=\sum_{1}^{n}(q_i+\Delta\Delta p_{\varphi i}\operatorname{tg}\bar{\alpha}_i). \tag{19}$$

Letting $p_{0(\tau)} = p_0 + \Delta p_{0(\tau)}$, and remembering that

$$\frac{F_0W_0p_0}{gR_0T_0}=q_\tau,\quad \frac{V_{ks}}{gR_0T_0}\frac{dp_0}{d\tau}=0, \tag{20}$$

we obtain a system of differential equations to describe the effective variations in mixture composition in terms of the variation in flow-rate for an n-component propellant in the presence of unsteady combustion manifested by pressure pulsation

$$\begin{aligned}
&A_{11}\frac{d\Delta p_{01(\tau)}}{d\tau}+A_{12}\Delta p_{01(\tau)}=\Delta\Delta p_{1(\tau-\tau_1)}\operatorname{tg}\bar{\alpha}_1,\\
&A_{21}\frac{d\Delta p_{02(\tau)}}{d\tau}+A_{22}\Delta p_{02(\tau)}=\Delta\Delta p_{2(\tau-\tau_2)}\operatorname{tg}\bar{\alpha}_2,\\
&\dots\dots\dots\dots\dots\dots\dots\dots\dots\dots,\\
&A_{n1}\frac{d\Delta p_{0n(\tau)}}{d\tau}+A_{2n}\Delta p_{0n(\tau)}=\Delta\Delta p_{n(\tau-\tau_n)}\operatorname{tg}\bar{\alpha}_n,
\end{aligned} \tag{21}$$

where

$$A_1=\frac{V_{ks}}{gR_0T_0},\quad A_2=\frac{F_0W_0}{R_0T_0},\quad \Delta\Delta p=\Delta p_{\varphi(\tau)}-\Delta p_{\varphi e}.$$

In accordance with the principle of superposition, the total pressure deviation in the combustion chamber will be a linear combination of all the deviations produced by the component disturbances:

$$\beta_1\Delta p_{01}+\beta_2\Delta p_{02}+\dots+\beta_n\Delta p_{0n}=\Delta p_{0(\tau)}. \tag{22}$$

We have thus solved the problem of space-time unsteady combustion. Let us now proceed to consider space-time-secondary unsteady combustion. This problem differs from the one just considered only that here the variation in flow-rate at the injector may be caused not only by disturbances in the propellant-supply system but also by disturbances stemming from the combustion chamber. The phenomenon of space-time-secondary unsteady combustion can be reduced to a certain closed system in which the initial coordinate $\Delta\Delta p$ affects the final coordinate Δp_0, and vice versa. On the basis of the well-known relationships for coordinate transformation, we have

$$L[\Delta p_{0(\tau)}]+P_{(s)}L[\Delta p_{0(\tau)}]=P_{(s)}L[\Delta\Delta p_{(\tau-t')}], \tag{23}$$

where $P_{(s)}$ is the transfer function for space-time-secondary unsteady combustion.

Applying the Duhamel integral to both products of the transfer function and to the $\Delta p_{0(\tau)}$ and $\Delta\Delta p_{(\tau-t')}$ transformation, we obtain:

$$P_{(s)}L[\Delta p_{0(\tau)}]=h_{(0)}\Delta p_{0(\tau)}+\int_0^{\tau}h'_{(t)}\Delta p_{0(\tau-t)}dt, \tag{24}$$

$$P_{(s)}L[\Delta\Delta p_{0(\tau-t')}]=h_{(0)}\Delta\Delta p_{(\tau)}+\int_0^{\tau}h'_{(t)}\Delta\Delta p_{(\tau-t)}dt, \tag{25}$$

where $h_{(0)}$ is a function of the pressure increment in the combustion chamber due to unit disturbance at the injector for $t = 0$, and $h'_{(t)}$ is the derivative of the function $h_{(t)}$.

Letting F_0 be the right side of Eq. (25), since it is a known function, and substituting the equations derived from the Duhamel integrals into Formula (23), we obtain

$$F_{0(\tau)}=\Delta p_{0(\tau)}[1+h_{(0)}]+\int_0^{\tau}h'_{(t)}\Delta p_{0(\tau-t)}dt, \tag{26}$$

or, dividing both sides by $1 + h_{(0)}$

$$F_{0(\tau)}=\Delta p_{0(\tau)}+\int_0^{\tau}J_{(t)}\Delta p_{(\tau-t)}dt, \tag{27}$$

where $F_{(t)} = F_{0(\tau)}/(1 + h_{(0)})$ is a known function depending on the pressure perturbation at the injector inlet, and $J_{(t)} = h'_{(t)}/(1 + h_{(0)})$ is a function depending on the pressure increment in the combustion chamber produced by a unit disturbance.

In the general case, for an n-component propellant, we have

$$F_{1(\tau)}=\Delta p_{01(\tau)}+\int_0^{\tau}J_{1(t)}\Delta p_{01(\tau-t)}dt,$$

$$F_{2(\tau)}=\Delta p_{02(\tau)}+\int_0^{\tau}J_{2(t)}\Delta p_{02(\tau-t)}dt, \tag{28}$$

$$\dots\dots\dots\dots\dots\dots\dots\dots\dots,$$

$$F_{n(\tau)} = \Delta p_{0n(\tau)} + \int_0^\tau J_{n(t)} \Delta p_{\ldots(\tau-t)}\, dt. \tag{28}$$

The resulting system of equations (28) is a system of Volterra integral equations of the second kind. It constitutes the solution to the problem of space-time-secondary unsteady combustion and is connected with the phenomenon of space-time unsteady combustion. If it turns out that sufficiently strong opposing disturbances occur, we can use this system of equations to examine the closed system, using the data for the open system. The equations mentioned can be solved by the method of successive approximations or the inverse Fourier transform. In the first case, the resolvent for the system of equations (28) will take the form

$$\begin{aligned}
\Delta p_{01(\tau)} &= F_{1(\tau)} + \lambda_1 \int_0^\tau H_{1(\tau,t,\lambda)} F_{1(t)}\, dt,\\
\Delta p_{02(\tau)} &= F_{2(\tau)} + \lambda_2 \int_0^\tau H_{2(\tau,t,\lambda)} F_{2(t)}\, dt,\\
&\dots\dots\dots\dots\dots\dots\dots\dots\dots,\\
\Delta p_{0n(\tau)} &= F_{n(\tau)} + \lambda_n \int_0^\tau H_{n(\tau,t,\lambda)} F_{n(t)}\, dt,
\end{aligned} \tag{29}$$

where $H_{(\tau,t,\lambda)} = \sum_{i=0}^{\infty} \lambda^i J_{i+1}(\tau, t)$ is the resolvent kernel, and λ is the eigenvalue.

It is quite difficult to determine exactly when space-time-secondary and space-time unsteady combustion occurs on the basis of the meager experimental studies. It is only certain that in the presence of strong disturbances, changes in the pressure inside the combustion chamber have a definite effect on the value of the pressure ahead of the injector. No such effect was found for very small combustion-process disturbances. The location of the boundary was not established. Numerous studies and investigations, primarily experimental, are required to settle this question.

4. ENGINE STARTUP PERIOD

An analysis of the available literature shows that damage to the propulsion assembly, frequently resulting in complete destruction of the engine, is caused primarily by improper choice of parameters for the initial operating period. Excessive propellant accumulation due to the large pressure drop across the injector during the initial startup phase produces a violent rise in chamber pressure. The actual pressure value may then exceed the calculated value by a factor that may even be greater than ten, and as a result the engine may sometimes fail. The solutions given in this chapter represent an attempt to give an analytical description of the phenomena occurring during startup. Let us examine the startup process for a liquid rocket engine using an n-component propellant. Assuming equal supply pressures

$$p_{s1(\tau)} = p_{s2(\tau)} = p_{s3(\tau)} = \dots = p_{sn(\tau)} \qquad (30)$$

we reduce this system of equations simultaneously to a single dynamic startup equation. Since temperature and pressure have the greatest affect on the change in load, and the relationship between these variables can be represented by simple formulas, we reduce the problem of the transition period to a study of the change in the pressure $p_{0(\tau)}$ alone. It has already been shown that the combustion chamber is a dynamic oscillating element. The oscillating nature of the chamber can be explained as follows: if the initial part of the load is greater than the calculated value, the pressure in the chamber following combustion will have a value higher than that predicted, and the pressure drop across the injector will thus decrease.

Fig. 2.

The decrease in $\Delta p_{g(\tau)}$ will reduce the load and thus $p_{0(\tau)}$ will drop below the calculated pressure value, again increasing $\Delta p_{g(\tau)}$. This process repeats itself, and if the damping forces are greater than the intensifying forces, the amplitude of the oscillations will decrease with time; if, on the other hand, the opposite is true, such pressure pulsations may cause the engine to fail. Since there exists a certain ignition lag $\underline{t}'$ between the time when the load is introduced into the chamber and the time at which it burns, the chamber pressure oscillations will shift with respect to the pulsation $\Delta p_{g(\tau)}$ by a certain angle corresponding to the time $\underline{t}'$.

The instant the load of propellant is introduced into the chamber, it burns, with a consequent pressure increase. If we assume that the mixture is uniform over the entire flame front, the force due to the uniformly propagating pressure will be proportional to the change in the slope tangent for $\Delta p_{g(\tau)}$. Since there is a strict functional relationship between $p_{0(\tau)}$ and $\Delta p_{g(\tau)}$, this force will be proportional to the second derivative of the chamber pressure with respect to time. If we also consider the amount and type of propellant load, we obtain the inertial forces

$$P_b = \frac{V_{ks}}{g}\frac{d^2 p_{0(\tau)}}{d\tau^2}. \qquad (31)$$

Both for damped pulsations as well as for oscillations of increasing amplitude, there exists a larger or smaller damping force proportional to the first derivative of the pressure. In general, this force will depend on the friction of the gas against the wall surface, R_s, the friction of the gas molecules, R_c, and the gas turbulence and counterflow, R_w. We therefore will have

$$P_t = (R_s + R_c + R_w)\frac{dp_{0(\tau)}}{d\tau}. \qquad (32)$$

Since there exists operating continuity during the transition period considered, there must also exist a force to initiate and ensure such continuity. This force originates in the very admission of the components into the combustion chamber, and its intensity will thus depend on the momentary propellant load. We can state that the thrust is proportional to the rate of flow of the components through the injector, with a certain negative lag $\underline{t}'$; hence

$$P_w = \frac{1}{kF_0}(\Delta p_{(\tau-t)}) \sum_1^{m'} f_i. \qquad (33)$$

where $\underline{k}$ is the thrust coefficient.

Combustion of a portion of the propellant causes a gas force to appear in the chamber; it depends on the pressure $p_{0(\tau)}$, the velocity $W(\tau)$, the flow-rate $G(\tau)$, and the chamber lateral dimension F_0

$$P_a = p_{0(\tau)} F_0 + F_0 \frac{\gamma}{g} \frac{\left(\int_{-T/2}^{T/2} \rho W_{(\tau)} d\tau\right)^2}{\left(\int_{-T/2}^{T/2} \rho d\tau\right)^2}. \qquad (34)$$

Ignoring the external forces acting on the engine, we obtain the dynamic differential equation for the transition period in the form

$$\frac{V_{ko}}{g} \frac{d^2 p_{0(\tau)}}{d\tau^2} + \frac{F_0 \gamma}{g} \frac{\left(\int_{-T/2}^{T/2} \rho W_{(\tau)} d\tau\right)^2}{\left(\int_{-T/2}^{T/2} \rho d\tau\right)^2} +$$

$$+(R_s+R_v+R_w)\frac{dp_{0(\tau)}}{d\tau} + p_{0(\tau)}F_0 - \frac{1}{k}\Delta p_{(\tau-t)} \sum_1^{m'} f_i = 0. \qquad (35)$$

If we confine the locus of thermal-parameter variation to the cross section with maximum pressure p_{0max}, we find that the velocity in this cross section is small, and we may thus assume that the gas force depends on the pressure alone. We simultaneously introduce the simple relationships for the flame-front volume; Eq. (35) then takes the form

$$\Theta_1^2 \frac{d^2 p_{0(\tau)}}{d\tau^2} + \Theta_2 \frac{dp_{0(\tau)}}{d\tau} + p_{0(\tau)} = \frac{\Delta p_{(\tau-t)}}{kF_0} \sum_1^{m'} f_i = 0. \qquad (36)$$

where

$$\theta_1 = \sqrt{\frac{t_0 G R_0 T_0}{g p_0 F_0}}, \quad \theta_2 = \frac{R_s + R_c + R_w}{F_0},$$

or, with the substitution $\tau = t\theta_1$

$$\frac{d^2 p_{0(\tau)}}{d\tau^2} + \frac{\theta_2}{2\theta_1} \frac{dp_{0(\tau)}}{d\tau} + p_{0(\tau)} = \frac{\Delta p_{z(\tau-\tau')}}{kF_0} \sum_1^m f_i. \tag{37}$$

The resulting Eq. (37), except for the singularity consisting in the earlier action of the thrust, has the properties of a sufficiently developed second-order linear differential equation. The coefficient <u>k</u> can be found from the formula

$$k = \frac{\Delta p_{z0} \sum_1^m f_i}{\sum_1^n G_i W_e} g. \tag{38}$$

Within the range of the linear functions, each change for $\sum_1^m f_i =$ const will produce a corresponding proportional change in the overall flow-rate $\sum_1^n G_i$. Since on the assumption p_0 = const the exhaust velocity W_e will not change, the coefficient <u>k</u> will also remain unchanged. Even if the difference in pressure across the injector should change owing to changes in p_0 alone, the result will be an automatic change in $\sum_1^n G_i$, which though not necessarily proportional to the variation $(p_z - p_0)$, would still leave <u>k</u> unchanged owing to the corresponding change in the exhaust velocity. Since an analysis of variation in the injector cross-sectional area leads to the same conclusion, we can say that the coefficient <u>k</u> will not vary even in the presence of a disturbed state. The value of <u>k</u> can also be found from the steady operation condition, using the formula

$$k = \frac{\Delta p_{z0} \sum_1^m f_i}{F_0 p_{00}}. \tag{39}$$

Let us now compare the factors in Eq. (36). If we reduce the chamber and nozzle damping-force factors to the pressure losses Δp for an equivalent pipe of diameter D and length L, represented with the aid of the Darcy-Weisbach relationships, the constants θ_1 and θ_2 will take the form

$$\frac{2L_{ns}D_{ns}\Delta p}{\overline{W}\overline{\gamma}F_0} \neq 2\sqrt{\frac{t_0 G R_0 T_0}{g p_0 F_0}}, \tag{40}$$

where $\overline{W}$ is the mean flow velocity and $\overline{\gamma}$ the mean gas specific gravity.

Expression (40) may be represented in the form

$$C_1\frac{\Delta p}{\overline{W}\overline{\gamma}} \neq 2C_2\sqrt{\frac{t_0 G T_0}{g F_0}}, \tag{41}$$

where

$$C_1 = \frac{2L_{ns}D_{ns}}{F_0}, \quad C_2 = \sqrt{\frac{R_0}{g F_0}}.$$

Using actual data for particular engine geometry, we find that for

$$C_1 \leqslant 2C_2, \tag{42}$$

the inequality

$$\frac{\Delta p}{\overline{W}\overline{\gamma}} < \sqrt{\frac{t_0 G T_0}{p_0}}. \tag{43}$$

will always hold.

In view of this Expression (40) will take on a definite mathematical form, important for all engines and applying to nearly every disturbance:

$$C_1\frac{\Delta p}{\overline{W}\overline{\gamma}} < 2C_2\sqrt{\frac{t_0 G T_0}{p_0}}. \tag{44}$$

It then follows that the solution for the dynamic startup equation takes the form of a product of exponential and trigonometric functions. Thus this confirms the conclusion that the combustion chamber is a dynamic oscillating element. The solution for Eq. (37) for unit disturbance is

$$p_{0(t)} = e^{-\alpha t}(A_1 \cos t\sqrt{1-\alpha^2} + A_2 \sin t\sqrt{1-\alpha^2}) + A_3, \tag{45}$$

where $\alpha = \theta_2/2\theta_1$.

We formulate the following initial conditions:

for t = 0

$$p_{0(t)} = 1, \quad p'_{0(t)} = p''_{0(t)} = 0, \tag{46}$$

for t = ∞ (steady engine operating range)

$$p_{0(t)} = \frac{1}{kF_0}(p_s - p_0)_{\rho\infty} \sum_1^{m'} f_i, \tag{47}$$

$$p'_{0(t)} = p''_{0(t)} = 0, \tag{48}$$

and we use these expressions to define the constants

$$A_1 = \frac{1}{kF_0}\left(kF_0 - \Delta p_{\rho\infty} \sum_1^{m'} f_i\right), \tag{49}$$

$$A_2 = \frac{\alpha}{\sqrt{1-\alpha^2}} - \frac{\alpha}{\sqrt{1-\alpha^2}}\left(\frac{1}{kF_0}\Delta p_{\rho\infty} \sum_1^{m'} f_i\right), \tag{50}$$

where

$$A_3 = \frac{1}{kF_0}\Delta p_{\rho\infty} \sum_1^{m'} f_i, \tag{51}$$

then the Solution (45) for Eq. (37) will take the form

$$\begin{aligned} p_{0(t)} = e^{-\alpha t}\Big[\frac{1}{kF_0}\left(kF_0 - \Delta p_{\rho\infty} \sum_1^{m'} f_i\right)\cos\sqrt{1-\alpha^2}\,t + \\ + \frac{\alpha}{\sqrt{1-\alpha^2}} - \frac{\alpha}{\sqrt{1-\alpha^2}}\left(\frac{1}{kF_0}\Delta p_{\rho\infty} \sum_1^{m'} f_i\right)\sin\sqrt{1-\alpha^2}\,t\Big] + \frac{1}{kF_0}\Delta p_{\rho\infty} \sum_1^{m'} f_i. \end{aligned} \tag{52}$$

Solution (52), thus formulated, describes the behavior of the pressure in the combustion chamber during a transition period. The smaller Θ_2 of the larger Θ_1, the greater the pulsation amplitudes will be. When a rocket motor is started, it is necessary for the chamber pressure to reach the design value rapidly, while not exceeding it. Experimental investigations have shown that during the transition periods, the pressure at the chamber intake will frequently pulsate. Since the curves involved approximate harmonic functions, we must study the behavior of the chamber pressure under such disturbances. We let

$$(p_z - p_0)_g(\tau - t') = (p_z - p_0)_a \sin\omega(\tau - t'). \tag{53}$$

then the solution of Eq. (36) for $\theta_2 < 2_{\theta 1}$ will take the form

$$p_{0(\tau)} = B_1 e^{-\alpha\tau/\theta_1}\sin\left(\sqrt{1-\alpha^2}\,\frac{\tau}{\theta_1} + B_2\right) + \frac{\Delta p_{ga}[\sin\omega(\tau - t' + \beta)]\sum_1^{m'} f_i}{F_0 k\sqrt{(1-\theta_1^2\omega^2)^2 + 4\theta_1^2\omega^2\alpha^2}}, \tag{54}$$

while for $\theta_2 > 2\theta_1$

$$p_{0(\tau)} = B_1 e^{-\alpha\tau/\theta_1}\sinh\left(\sqrt{1-\alpha^2}\,\frac{\tau}{\theta_1} + B_2\right) + \frac{\Delta p_{ga}[\sin\omega(\tau - t' + \beta)]\sum_1^{m'} f_i}{F_0 k\sqrt{(1-\theta_1^2\omega^2)^2 + 4\theta_1^2\omega^2\alpha^2}}. \tag{55}$$

If $\tau = \infty$, Eq. (54) and (55) will be identical in form. From this it follows that the effect of the ratio $\theta_2/2\theta_1$ on $p_{0(\;)}$ for a sinusoidal change in $(p_z - p_0)_g$ is of no importance. Whatever the ratio of the constants θ_1 and θ_2, for this type of variation in the pressure drop across the injector, the combustion-chamber pressure will be represented by the function

$$p_{0(\tau)} = \frac{\Delta p_{ga}[\sin(\tau - t' + \beta)]\sum_1^{m'} f_i}{kF_0\sqrt{(1-\theta_1^2\omega^2) + 4\theta_1^2\omega^2\alpha^2}}. \tag{56}$$

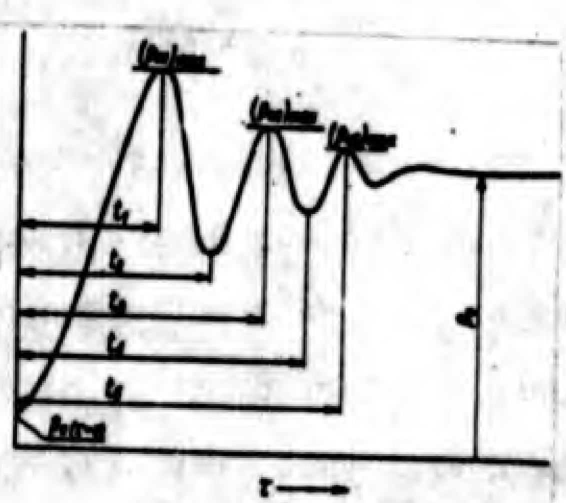

Fig. 3.

Let us now determine the engine optimum and critical parameters on the basis of the startup curves. It is known that engine failure results primarily from an abrupt rise in chamber pressure during startup. Owing to the accumulation of an excessive amount of propellant, the chamber will burst at the initial pressure maximum. Setting the first derivative of Eq. (45) equal to zero, we obtain the times at which the pressure $p_0(t)$ reaches the extremum values (Fig. 3)

$$\sin\sqrt{1-\alpha^2}\,t = 0, \tag{57}$$

$$t_n = \frac{\pi n}{\sqrt{1-\alpha^2}}. \tag{58}$$

For the first maximum $p_{0(t)}$, we have

$$t_1 = \frac{\pi}{\sqrt{1-\alpha^2}} \tag{59}$$

and

$$p_{0(t)\max} = e^{-\alpha\pi/\sqrt{1-\alpha^2}}\left[\frac{1}{kF_0}\left(kF_0 - \Delta p_{pr}\sum_1^{m'} f_i\right)\right] + \frac{1}{kF_0}\Delta p_{pr}\sum_1^{m'} f_i. \tag{60}$$

Using the prescribed chamber safety factor n_0, we obtain the critical value for the pressure drop across the injector nozzle

$$\Delta p_{kr} = \frac{n_0 p_{0\,ob1} - e^{-\alpha\pi/\sqrt{1-\alpha^2}}}{\frac{1}{kF_0}\sum_1^{m} f_i\left(1 - e^{-\alpha\pi/\sqrt{1-\alpha^2}}\right)}\, e^{-\alpha\tau'}. \tag{61}$$

As we know, however, in selecting engine specifications, we are interested primarily in the values of the optimum parameters such as Δp_{opt}, $p_{0_{opt}}$, $V_{ks\ opt}$. It is necessary to determine the propulsion-system startup regime for which the pressure in the combustion chamber will rise gradually to the design value. On the other hand, the time required for $p_0 = 1$ to reach $p_0 = p_{ob1}$ must be as brief as possible. The problem of determining optimum startup parameters can therefore be reduced to finding the minimum energy increment between the steady-pressure energy and the variable-pressure energy over the transition period. We can solve this problem by integration. We obtain the minimum energy increment when the integral for the pressure drop $p_0 - p_{0(t)}$ reaches its minimum value. If at startup we have n extremum values for the function $p_0 = f(t)$, we will have smooth startup for the case $\theta_2 < 2\theta_1$ when

$$\int_0^{\infty}\left|e^{-\alpha t}\left\{\frac{1}{kF_0}\left(kF_0-\Delta p_{0m}\sum_{1}^{m'}f_i\right)\cos\sqrt{1-\alpha^2}\,t+\right.\right.$$
$$\left.\left.+\left[\frac{\alpha}{\sqrt{1-\alpha^2}}-\frac{\alpha}{\sqrt{1-\alpha^2}}\left(\frac{1}{kF_0}\Delta p_0\sum_{1}^{m'}f_i\right)\right]\sin\sqrt{1-\alpha^2}\,t\right\}dt\right| = \min. \tag{62}$$

It can be shown that the value of Integral (62) depends on α, and hence primarily on the engine parameters (p_0, G, F_0) and the propellant parameters (T_0, R_0, t_0). If this is the case, then for a given fuel and oxidizer, and for a given engine size, we can uniquely determine the pressure in the combustion chamber. We find the optimum values α_{opt} (Fig. 4) for the minimum of the integral $\int_0^{\infty}|p_0-p_{0(t)}dt|$ and hence p_{0opt}:

$$p_{0opt} = \frac{\alpha^2 4 t_0 G R_0 T_0 F_0}{R^2 g}. \tag{63}$$

Fig. 4.

As we know, no precise criterion for the selection of combustion-chamber pressure has so far been stated even for the classical engines with de Laval nozzles. The available textbooks merely recommend values between 15 and 45 kgf/cm^2. The argument just presented can therefore be used as a basis for one possible definition to be used in selecting chamber pressure from the viewpoint of smooth startup. Determination of the optimum value $p_{0_{opt}}$ would permit more precise determination of other chamber parameters, in particular the volume and length of the combustion chamber. The introduction of this criterion, however, involves certain difficulties in view of the necessity of determining the duration of the first half cycle of pressure oscillation in the combustion chamber. On the other hand, it is known that this time is roughly twice the combustion time. Since the latter can be determined for a given propellant, we can also determine t_1 in approximation. This is not a very accurate method, however. Another way of determining α_{opt} consists in establishing its range of variation. Using Eq. (58) and the formula for half-cycle duration

$$t_n = \frac{1}{\sqrt{1-\alpha^2}}\left(n\pi - \operatorname{arctg}\frac{\sqrt{1-\alpha^2}}{\alpha}\right) \qquad (64)$$

the relationships $\int_0^\infty |p_0 - p_{0(t)} dt| = f(\alpha)$ were found for four different transition periods. It follows from the graphs of Fig. 5 that the minimum value of this function will be shifted toward α as the number of half-cycles increases. At the same time, we can see that the derivative of the curve A-B, representing the sets of minimums, becomes increasingly larger, thus indicating a constantly diminishing range of variation in α_{opt} as the number of half-cycles is increased. We therefore have a basis for restricting the range of α to the limits 0.61-0.675. We know, however, that if a pressure deviation occurs there must be at least two half cycles, and for this reason the curve for one half cycle cannot be considered. Hence the range of variation in α_{opt} will be narrower, with limits 0.66-0.68. It follows from the distribution in Fig. 5 that for more than four half cycles, the increment in α_{opt} will be small.

By finding α_{opt}, we can find the optimum pressure in the combustion chamber. This is essential in the design of a rocket propulsion

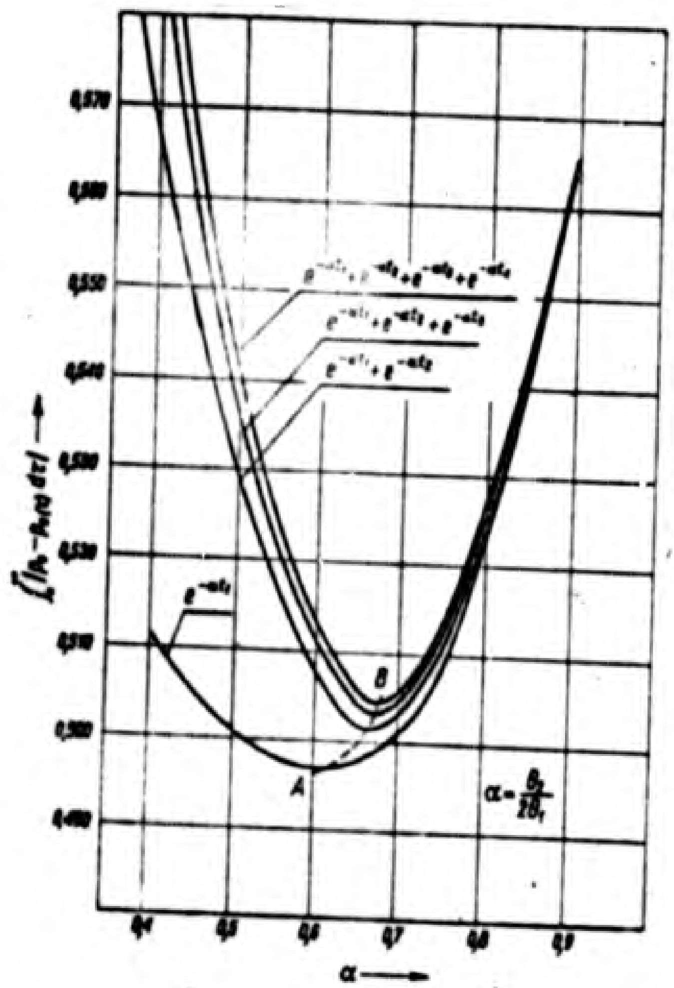

Fig. 5.

system. In an analysis, we are usually concerned with a particular engine, and we carry out studies to determine its characteristics. Here it is necessary to obtain the engine startup curve – the so-called pressure simulation curve for the chamber – from which it is possible to evaluate the initial engine performance. The curve must be so shaped as to give the shortest possible time of transition from atmosphere pressure to the combustion-chamber design pressure. On the other hand, the curve must also be smooth. Such a curve can be obtained by minimizing the quadratic form of the variables characterizing the transition-period performance. If we let

$$\eta_{(\tau)} = p_0 - p_{0(\tau)}, \tag{65}$$

the dynamic equation (36) will take the form

$$\Theta_1^2 \frac{d^2\eta_{(\tau)}}{d\tau^2} + \Theta_2 \frac{d\eta_{(\tau)}}{d\tau} + \eta_{(\tau)} = \frac{(p_s - p_0)_{(\tau - \tau_i)}}{kF_0} \sum_1^n f_i. \tag{66}$$

Allowing for the fact that the engine performance will be characterized primarily by the first derivative and the function $\eta_{(\tau)}$, we look for the minimum of the quadratic form

$$J = \int_0^\infty |V_{(\tau)} d\tau|_{\min} = \left[\int_0^\infty \theta_2 \left(\frac{d\eta_{(\tau)}}{d\tau}\right)^2 + (\eta_{(\tau)})^2 d\tau\right]_{\min}. \qquad (67)$$

If there is a function $V_{(\tau)}$ such that the integral J takes on an extremum value, the function must be a solution for the Euler variational equation

$$\frac{\partial V}{\partial \eta} - \frac{d}{d\tau}\frac{\partial V}{\partial \eta'} = 0. \qquad (68)$$

We thus obtain the equation

$$\theta_2^2 \frac{d^2\eta_{(\tau)}}{d\tau^2} - \eta_{(\tau)} = 0, \qquad (69)$$

whose solution

$$\eta_{(\tau)} = B_1 e^{-\tau/\theta_2} + B_2 e^{-\tau/\theta_2} \qquad (70)$$

defines the startup process with minimum pressure energy loss. Equation (70) is used to determine the pressure difference $p_0 - p_0(t)$ for which the combustion-chamber pressure will rise smoothly but reach the design value within a fairly short time. For the following initial conditions:

for $\tau = 0$

$$\eta_{(0)} = p_0 - 1, \qquad (71)$$

for $t = \infty$

$$\lim_{t \to \infty} \eta = 0 \qquad (72)$$

we have

$$B_1 = p_0 - 1, \quad B_2 = 0. \qquad (73)$$

The solution will then take the form

$$\eta_{(\tau)} = (p_0 - 1)e^{-\tau/\theta_2}. \qquad (74)$$

Investigation of engine startup was carried out only for the case $\Theta_2 < 2\Theta_1$. It is easy to show that for cases in which $\Theta_2 \geq 2\Theta_1$ where, as we know, the dynamic equation (36) has a corresponding solution:

for $\theta_2 = 2\theta_1$

$$p_{0(t)} = (C_1 + tC_2)e^{-t} + C_3, \qquad (75)$$

for $\theta_2 > 2\theta_1$

$$p_{0(t)} = D_1 e^{\lambda_1 t} + D_2 e^{\lambda_2 t}, \qquad (76)$$

and Integral (62) does not have a minimum but increases with the average increase of θ_2 over $2\theta_1$. The minimum for this integral lies in the range $0 < \alpha < 1$, and the optimum parameters must be found exclusively with this range.

5. STUDY OF TRANSIENTS IN PROPELLANT-SUPPLY SYSTEM

The entire supply system was divided into n lines with one common combustion chamber (Fig. 6). Where there is a pressure accumulator, each propellant line is made up of an accumulator, reduction system, tank, cooling chamber, and injector. Where turbopump pressurization is used, we have the generator system and the pumps in place of the pressure accumulator. This chapter will be concerned in particular with the

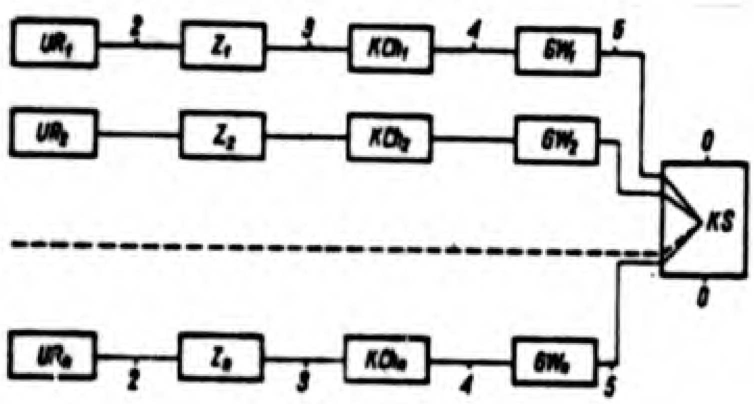

Fig. 6.

pressurized supply system. The individual elements will be replaced by dynamic elements (Fig. 6) described by means of dynamic differential equations.

Assuming an isentropic gas flow through the reduction valves and pressure increments proportional to the first derivative of the specific gravity with respect to time, we obtain a system of equations for the various reduction systems:

$$\Theta_1'' \frac{d\Delta p_{12(\tau)}}{d\tau} + \Delta p_{12(\tau)} = -B_1 \Delta p_{11(\tau)},$$

$$\Theta_2'' \frac{d\Delta p_{22(\tau)}}{d\tau} + \Delta p_{22(\tau)} = -B_2 \Delta p_{21(\tau)},$$

$$\ldots\ldots\ldots\ldots\ldots\ldots\ldots\ldots\ldots,$$

$$\Theta_n'' \frac{d\Delta p_{n2(\tau)}}{d\tau} + \Delta p_{n2(\tau)} = -B_n \Delta p_{n1(\tau)}, \qquad (77)$$

where $\Theta'' = b/RT$, b is the coefficient for the change in specific gravity, B is a reduction-valve structural parameter, and Δp_2 is the pressure increment after the reduction valve.

Disturbances passing through the accumulator and entering the reducing system can be classified into three basic groups:

1) disturbances of unit character,

2) disturbances of pulsation nature, represented in the basic case by means of the following Fourier equations:

$$\Delta p_{11(\tau)} = \left(\sum_{n=1}^{\infty} A_n \sin n\omega\tau + \sum_{n=1}^{\infty} B_n \cos n\omega\tau\right)_1,$$

$$\Delta p_{21(\tau)} = \left(\sum_{n=1}^{\infty} A_n \sin n\omega\tau + \sum_{n=1}^{\infty} B_n \cos n\omega\tau\right)_2, \qquad (78)$$

$$\ldots\ldots\ldots\ldots\ldots\ldots\ldots\ldots\ldots,$$

$$\Delta p_{n1(\tau)} = \left(\sum_{n=1}^{\infty} A_n \sin n\omega\tau + \sum_{n=1}^{\infty} B_n \cos n\omega\tau\right)_n.$$

3) disturbances of random nature:

$$\Delta p_{11(\tau)} = \Psi_1(e^{-\tau}, \cos\omega\tau, \sin\omega\tau),$$

$$\Delta p_{21(\tau)} = \Psi_2(e^{-\tau}, \cos\omega\tau, \sin\omega\tau), \qquad (79)$$

$$\ldots\ldots\ldots\ldots\ldots\ldots\ldots\ldots\ldots,$$

$$\Delta p_{n2(\tau)} = \Psi_n(e^{-\tau}, \cos\omega\tau, \sin\omega\tau).$$

In order to derive formulas to describe the turbulent fluid flow between sections (2-2) and (3-3) of Fig. 7, we shall employ the principle of energy variation in the volume under consideration. This energy change represents the sum of the external work and internal work of the system

$$\frac{\partial}{\partial\tau} E d\tau = \frac{\partial}{\partial\tau} L d\tau = \left(\frac{\partial}{\partial\tau} L_{\text{внеш}} + \frac{\partial}{\partial\tau} L_{\text{внут}}\right) d\tau. \qquad (80)$$

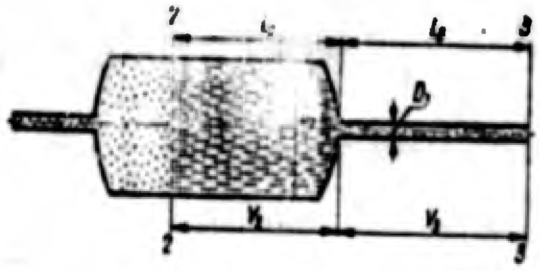

Fig. 7.

On the other hand, the kinetic-energy increment can be represented as the sum of the energy inside this value and the energy at its surface S

$$\frac{\partial}{\partial\tau}E\,d\tau = \frac{\gamma}{2g}\left[\int_V \frac{\partial}{\partial\tau}(W)^2 dV + \int_S (W)^2 V_n dS\right]d\tau. \qquad (81)$$

If we divide the entire investigated component volume between the indicated sections into n parts or even into several characteristic volumes, and go from the integral to the sum, we obtain

$$\frac{\gamma}{2g}\left[\int_V \frac{\partial}{\partial\tau}(W)^2 dV\right]d\tau = \frac{\gamma}{2g}\left[V_2\frac{\partial}{\partial\tau}(W_2)^2 d\tau + V_3\frac{\partial}{\partial\tau}(W_3)^2 d\tau\right]. \qquad (82)$$

$$\frac{\gamma}{2g}\left[\int_S (W)^2 V_n dS\right]d\tau = \frac{G}{2g}(W_3^2 - W_2^2)d\tau. \qquad (83)$$

The work done by the internal forces can be represented as the sum of the losses due to friction and the fluid pressure forces, represented in terms of kinematic quantities

$$\frac{\partial}{\partial\tau}(L_{\text{[illegible]}})d\tau = \frac{G}{\gamma}(p_2 - p_3)d\tau - R_2W_2d\tau - R_3W_3d\tau. \qquad (84)$$

Letting

$$\frac{\partial}{\partial\tau}(L_{\text{[illegible]}})d\tau = 0, \quad R = \zeta\frac{\rho W^2}{2}\frac{lF}{D} \qquad (85)$$

and substituting the resulting expressions into Eq. (80), we obtain

$$\frac{l_2}{g}\frac{dW_2}{d\tau} + \left[\zeta\frac{l_2}{2gD_2} - \frac{1}{2g}\right]W_2^2 - \frac{p_2}{\gamma} = \frac{l_3}{g}\frac{dW_3}{d\tau} - \left[\zeta\frac{l_3}{2gD_3} - \frac{1}{2g}\right]W_3^2 - \frac{p_3}{\gamma}. \qquad (86)$$

In view of the fact that the mean thrust is constant, we can reduce the problem under investigation to a linear problem. Applying small-perturbation theory and linearizing the function $W = \psi(p)$ with the aid of the Taylor formula, we finally obtain a dynamic differential equation describing the disturbed state in the tank:

$$\bar{\theta}^{*}\frac{d\Delta p_{2(t)}}{d\tau}+\varkappa^{*}\Delta p_{2(t)} = -\theta^{**}\frac{d\Delta p_{3(t)}}{d\tau}+\Delta p_{3(t)}, \tag{87}$$

where

$$\bar{\theta}^{*} = \frac{\frac{l_2}{g}\frac{\partial W_2}{\partial p_2}}{-\zeta\frac{l_3}{2gD_3}\frac{\partial W_3}{\partial p_3}\overline{W}_3+\frac{1}{g}\frac{\partial W_3}{\partial p_3}\overline{W}_3+\frac{1}{\gamma}}, \tag{88}$$

$$\theta^{**} = \frac{-\frac{l_3}{g}\frac{\partial W_3}{\partial p_3}}{-\zeta\frac{l_3}{2gD_3}\frac{\partial W_3}{\partial p_3}\overline{W}_3+\frac{1}{g}\frac{\partial W_3}{\partial p_3}\overline{W}_3+\frac{1}{\gamma}}, \tag{89}$$

$$\varkappa^{*} = \frac{\zeta\frac{l_2}{2gD_2}\frac{\partial W_2}{\partial p_2}\overline{W}_2-\frac{1}{g}\frac{\partial W_2}{\partial p_2}\overline{W}_2+\frac{1}{\gamma}}{-\zeta\frac{l_3}{2gD_3}\frac{\partial W_3}{\partial p_3}\overline{W}_3+\frac{1}{g}\frac{\partial W_3}{\partial p_3}\overline{W}_3+\frac{1}{\gamma}}. \tag{90}$$

For the n components of the propellant, the system of equations (87) will take the form

$$\begin{aligned}
&\bar{\theta}_1^{*}\frac{d\Delta p_{21}}{d\tau}+\varkappa_1^{*}\Delta p_{21} = -\theta_1^{**}\frac{d\Delta p_{31}}{d\tau}+\Delta p_{31},\\
&\bar{\theta}_2^{*}\frac{d\Delta p_{22}}{d\tau}+\varkappa_2^{*}\Delta p_{22} = -\theta_2^{**}\frac{d\Delta p_{32}}{d\tau}+\Delta p_{32},\\
&\dots\dots\dots\dots\dots\dots\dots\dots\dots\dots,\\
&\bar{\theta}_n^{*}\frac{d\Delta p_{2n}}{d\tau}+\varkappa_n\Delta p_{2n} = -\theta_n^{**}\frac{d\Delta p_{3n}}{d\tau}+\Delta p_{3n}.
\end{aligned} \tag{91}$$

The equation for turbulent flow through the cooling chamber can be derived by means of the Bernoulli law. Taking into account the heat transferred to the liquid through the internal wall from the gases and the heat transferred out through the external chamber wall (Fig. 8),

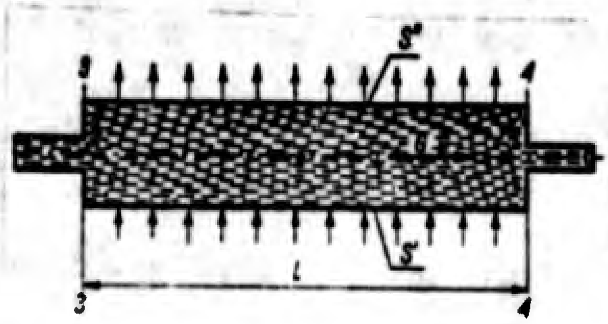

Fig. 8.

this equation will take the form

$$\frac{W_3^2}{2g}+\frac{p_3}{\gamma}=\frac{W_4^2}{2g}+\frac{p_4}{\gamma}+\sum_{1}^{n}h_i+\frac{1}{g}\int_{3}^{4}\frac{\partial W_s}{\partial \tau}dS+$$

$$-\frac{\lambda'}{\bar{Q}A}\int_{0}^{\tau_1}\int_{S'}\frac{\partial T}{\partial n}dS'd\tau+\frac{\lambda'}{\bar{Q}A}\int_{0}^{\tau_1}\int_{S''}\frac{\partial T}{\partial n}dS''d\tau, \tag{92}$$

where S is the transverse cross-sectional area of the cooling chamber, S' is the external-wall surface field, S" is the internal-wall surface field, n is the direction of the normal to S' or S", λ' is the conduction coefficient, $\bar{Q}\,\Big|_0^{\tau_1}=\int G d\tau$, and h is the cooling-chamber friction loss.

The change in energy produced by the fluid inertial forces during a disturbance, when the problem becomes one in axial flow, can be represented as

$$\frac{1}{g}\int_{3}^{4}\frac{\partial W_s}{\partial \tau}dS=\frac{l}{g}\left(\frac{dW_4}{d\tau}-\frac{dW_3}{d\tau}\right). \tag{93}$$

The energy increment produced for the liquid by the heat influx can be represented as the difference in the heat energy entering through wall S" and the heat energy leaving through S', and associated with the heat flows

$$\frac{\lambda'}{\bar{Q}A}\left(\int_{0}^{\tau_1}\int_{S''}\frac{\partial T}{\partial n}dS''d\tau-\int_{0}^{\tau_1}\int_{S'}\frac{\partial T}{\partial n}dS'd\tau\right)=\frac{\gamma V C_p}{\bar{Q}A}(\Delta T_{S''}-\Delta T_{S'}). \tag{94}$$

where V is the cooling-chamber volume, C_p is the specific heat at constant pressure, $\Delta T_{S'}$ is the difference between the temperatures of the outer wall and the coolant, $\Delta T_{S''}$ is the difference in the temperatures of the inner wall and the coolant, $\underline{l}$ is the length of the cooling chamber, and q_S is the unit heat flow.

Substituting the resulting expression into Eq. (92), we obtain a dynamic differential equation describing the turbulent liquid flow in the cooling chamber

$$\frac{W_3^2}{2g}+\frac{p_3}{\gamma}=\frac{W_4^2}{2g}+\frac{p_4^3}{\gamma}+\zeta\frac{W_{tr}}{2g}+\frac{1}{g}\left(\frac{dW_4}{d\tau}-\frac{dW_3}{d\tau}\right)+\frac{\gamma VC_p}{\overline{Q}A}(\Delta T_{S''}-\Delta T_{S'}) \tag{95}$$

or, after reducing the function W = ψ(p) to a linear relationship

$$\bar{\theta}''\frac{d\Delta p_{3(\tau)}}{d\tau}+\varkappa''\Delta p_{3(\tau)}=\theta'''\frac{d\Delta p_{4(\tau)}}{d\tau}+\Delta p_{4(\tau)}, \tag{96}$$

where

$$\varkappa''=\frac{\frac{\partial W_3}{\partial p_3}\frac{W_3}{g}+\frac{1}{\gamma}-\frac{\zeta}{4g}\frac{\partial W_3}{\partial p_3}-\frac{\zeta}{4g}\frac{\partial W_3}{\partial p_3}\overline{W}_4}{\frac{\partial W_4}{\partial p_4}\frac{\overline{W}_4}{g}+\frac{1}{\gamma}+\frac{\zeta}{4g}\frac{\partial W_4}{\partial p_4}+\frac{\zeta}{4g}\frac{\partial W_4}{\partial p_4}\overline{W}_3+\frac{\gamma F_4 C_p}{2GA}\frac{\partial W_4}{\partial p_4}(\Delta T_{S''}-\Delta T_{S'})}, \tag{97}$$

$$\bar{\theta}''=\frac{\frac{l}{g}\frac{\partial W_3}{\partial p_3}}{\frac{\partial W_4}{\partial p_4}\frac{\overline{W}_4}{g}+\frac{1}{\gamma}+\frac{\zeta}{4g}\frac{\partial W_4}{\partial p_4}+\frac{\zeta}{4g}\frac{\partial W_4}{\partial p_4}\overline{W}_3+\frac{\gamma F_4 C_p}{2GA}\frac{\partial W_4}{\partial p_4}(\Delta T_{S''}-\Delta T_{S'})}, \tag{98}$$

$$\theta'''=\frac{\frac{l}{g}\frac{\partial W_4}{\partial p_4}}{\frac{\partial W_4}{\partial p_4}\frac{\overline{W}_4}{g}+\frac{1}{\gamma}+\frac{\zeta}{4g}\frac{\partial W_4}{\partial p_4}+\frac{\zeta}{4g}\frac{\partial W_4}{\partial p_4}\overline{W}_3+\frac{\gamma F_4 C_p}{2GA}\frac{\partial W_4}{\partial p_4}(\Delta T_{S''}-\Delta T_{S'})}. \tag{99}$$

As a rule, the rocket motor uses one or sometimes two propellant components as coolants. In exceptional cases, three components may be used for cooling. Thus, if we generalize the problem under study, the system of equations of Type (96) will take the form

$$\bar{\theta}_1''\frac{d\Delta p_{31}}{d\tau}+\varkappa''\Delta p_{31}=\theta'''\frac{d\Delta p_{41}}{d\tau}+\Delta p_{41}, \tag{100}$$

$$
\begin{gathered}
\overline{\theta}_2^{\prime\prime}\frac{d\Delta p_{32}}{d\tau}+\varkappa_2^{\prime\prime}\Delta p_{32}=\theta^{\prime\prime}\frac{d\Delta p_{42}}{d\tau}+\Delta p_{42},\\
\dots\dots\dots\dots\dots\dots\dots\dots\dots,\\
\overline{\theta}_n^{\prime\prime}\frac{d\Delta p_{3n}}{d\tau}+\varkappa_n^{\prime\prime}\Delta p_{3n}=\theta_n^{\prime\prime}\frac{d\Delta p_{4n}}{d\tau}+\Delta p_{4n}.
\end{gathered}
\tag{100}
$$

Turbulent flow of the liquid through the injector, assuming equal pressures in the combustion chamber and the injector exit, is the same as space-time unsteady combustion. Thus this flow can be described with the aid of a system of differential equations with the lagging argument

$$
\begin{gathered}
\theta_1^{\prime}\frac{d\Delta p_{31}}{d\tau}+\Delta p_{31}=\varkappa_1^{\prime\prime}\Delta p_{41}(\tau-t'),\\
\theta_2^{\prime}\frac{d\Delta p_{32}}{d\tau}+\Delta p_{32}=\varkappa_2^{\prime\prime}\Delta p_{42}(\tau-t'),\\
\dots\dots\dots\dots\dots\dots\dots\dots\dots,\\
\theta_n^{\prime}\frac{d\Delta p_{3n}}{d\tau}+\Delta p_{3n}=\varkappa_n^{\prime\prime}\Delta p_{4n}(\tau-t'),
\end{gathered}
\tag{101}
$$

where

$$
\varkappa^{\prime\prime}=\frac{(\operatorname{tg}\overline{\alpha})R_0T_0}{W_0F_0},\quad \theta^{\prime}=\frac{A_1}{A_2},\quad \Delta p_4=\Delta\Delta p_g. \tag{102}
$$

The systems of equations derived for the fundamental dynamic elements make it possible to consider unsteady operation of these elements under arbitrary disturbances. These considerations refer to a rocket motor with pressurized propellant supply. In considering disturbed states with a turbopump supply, the system of equations for the reduction elements may be discarded, but it is then necessary to derive the differential equations for the catalyst and turbopump systems, which does not present any particular difficulty.

Using the systems of dynamic differential equations constructed, we can study the characteristics of the individual elements in isolation. It is difficult, however, to trace the propagation of disturbances from, for example, the accumulator to the combustion chamber. It is far more convenient to determine disturbance propagation through the lines by a functional relationship connecting the parameters at the reduction-system input and the combustion-chamber internal parameters. Such a relationship can be established by eliminating the individual variables in the equation systems (77), (91), (100) and (101). We thus obtain

$$\begin{gathered}
\bar{A}_1 \frac{d^4\Delta p_{01}}{d\tau^4} + \bar{B}_1 \frac{d^3\Delta p_{01}}{d\tau^3} + \bar{C}_1 \frac{d^2\Delta p_{01}}{d\tau^2} + \bar{D}_1 \frac{d\Delta p_{01}}{d\tau} + \Delta p_{01} = \\
= \left(\bar{E}_1 \frac{d^2\Delta p_{11}}{d\tau^2} + \bar{F}_1 \frac{d\Delta p_{11}}{d\tau} + \bar{G}_1 \Delta p_{11}\right) e^{-\sigma\tau}, \\
\bar{A}_2 \frac{d^4\Delta p_{02}}{d\tau^4} + \bar{B}_2 \frac{d^3\Delta p_{02}}{d\tau^3} + \bar{C}_2 \frac{d^2\Delta p_{02}}{d\tau^2} + \bar{D}_2 \frac{d\Delta p_{02}}{d\tau} + \Delta p_{02} = \\
= \left(\bar{E}_2 \frac{d^2\Delta p_{12}}{d\tau^2} + \bar{F}_2 \frac{d\Delta p_{12}}{d\tau} + \bar{G}_2 \Delta p_{12}\right) e^{-\sigma\tau}, \\
\cdots\cdots\cdots\cdots\cdots\cdots\cdots\cdots\cdots\cdots\cdots\cdots\cdots\cdots, \\
\bar{A}_n \frac{d^4\Delta p_{0n}}{d\tau^4} + \bar{B}_n \frac{d^3\Delta p_{0n}}{d\tau^3} + \bar{C}_n \frac{d^2\Delta p_{0n}}{d\tau^2} + \bar{D}_n \frac{d\Delta p_{0n}}{d\tau} + \Delta p_{0n} = \\
= \left(\bar{E}_n \frac{d^2\Delta p_{1n}}{d\tau^2} + \bar{F}_n \frac{d\Delta p_{1n}}{d\tau} + \bar{G}_n \Delta p_{1n}\right) e^{-\sigma\tau},
\end{gathered} \tag{103}$$

where

$$\begin{aligned}
\bar{A} &= \theta'\theta''\theta'''\theta'''', \\
\bar{B} &= \theta'\theta''\theta''' + \theta'\theta''\theta'''' + \theta'\theta'''\theta'''' + \theta''\theta'''\theta'''', \\
\bar{C} &= \theta'\theta'' + \theta'\theta''' + \theta'\theta'''' + \theta''\theta''' + \theta''\theta'''' + \theta'''\theta'''', \\
\bar{D} &= \theta' + \theta'' + \theta''' + \theta'''', \\
\bar{E} &= x'''\bar{B}\theta'\bar{\theta}'', \\
\bar{F} &= x'''B(\bar{\theta}'x'' + \bar{\theta}''x'), \\
\bar{G} &= x'x''x'''B.
\end{aligned}$$

This system of dynamic differential equations describes the disturbed states of engine operation; each equation refers to one line for one propellant component. Where there are more than 4 elements in a single line, the order of the equation will increase, while if there are fewer elements, the order of the equation will be reduced accordingly. From the mathematical standpoint, solution of this equation system is not difficult, but it is time consuming. For this reason, it is more convenient to reduce these equations to an operator transfer function or to the Heaviside operator ($d/d\tau = S$). Then for an open system we have

$$\begin{aligned}\bar{P}_{1(S)} &= P_{11(S)}P_{12(S)}P_{13(S)}P_{14(S)},\\ \bar{P}_{2(S)} &= P_{21(S)}P_{22(S)}P_{23(S)}P_{24(S)},\\ &\dots\dots\dots\dots,\\ \bar{P}_{n(S)} &= P_{n1(S)}P_{n2(S)}P_{n3(S)}P_{n4(S)},\end{aligned} \tag{104}$$

where $P_{1(S)} = B/(\theta''S + 1)$ is the transfer function for the reduction system, $P_{2(S)} = \frac{\bar{\theta}'S+\varkappa'}{\theta''S+1}$ is the transfer function for the tank,

$P_{3(S)} = \frac{\bar{\theta}''S+\varkappa''}{\theta''S+1}$ is the transfer function for the cooling chamber,

$P_{4(S)} = \frac{\varkappa'''e^{-\varkappa t}}{\theta'S+1}$ is the transfer function for the injector.

With certain propellant-supply system designs or under strong disturbances, the opposite effect may occur. The system of operator equations will then take the form

$$\begin{aligned}\bar{P}_{1(S)} &= \frac{P_{11(S)}}{1+P_{11(S)}H_{11(S)}} + \frac{P_{12(S)}}{1+P_{12(S)}H_{12(S)}} + \frac{P_{13(S)}}{1+P_{13(S)}H_{13(S)}} + \frac{P_{14(S)}}{1+P_{14(S)}H_{14(S)}},\\ \bar{P}_{2(S)} &= \frac{P_{21(S)}}{1+P_{21(S)}H_{21(S)}} + \frac{P_{22(S)}}{1+P_{22(S)}H_{22(S)}} + \frac{P_{23(S)}}{1+P_{23(S)}H_{23(S)}} + \frac{P_{24(S)}}{1+P_{24(S)}H_{24(S)}},\\ &\dots\dots\dots\dots,\\ \bar{P}_{n(S)} &= \frac{P_{n1(S)}}{1+P_{n1(S)}H_{n1(S)}} + \frac{P_{n2(S)}}{1+P_{n2(S)}H_{n2(S)}} + \frac{P_{n3(S)}}{1+P_{n3(S)}H_{n3(S)}} + \frac{P_{n4(S)}}{1+P_{n4(S)}H_{n4(S)}},\end{aligned} \tag{105}$$

where H(S) is the operator function for the opposite reaction.

The operator transfer functions offer a more convenient way of studying a disturbed state, both for a single dynamic element and for many such elements. The suitable arrangement of transfer functions immediately gives us the form of the final coordinate for a particular form of disturbance. As an example, let us consider disturbances in an open supply system for a monopropellant. If the disturbance appears ahead of the combustion chamber, in unit form, then when

$$P_{11(S)}P_{12(S)}P_{13(S)} = \mathrm{const}, \tag{106}$$

$$\bar{P}_{1(S)} = \mathrm{const}\,\frac{\varkappa'''e^{-\varkappa t}}{\theta'S+1} \tag{107}$$

we have a combustion-chamber pressure deviation of the form

$$\Delta p_{0(\tau)} = \Delta p_1 \, \mathrm{const} \, \varkappa'''\left(e^{-\tau'/\theta'''} - e^{-(1/\theta''')(\tau+\tau')}\right). \tag{108}$$

A more interesting case results from a unit disturbance supplied to the duct containing the "exiting" gas ahead of the reduction valve. The change of pressure following the reduction system will be described by the expression

$$\Delta p_{2(\tau)} = \Delta p_1 B\left(1 - e^{-\tau/B}\right), \tag{109}$$

after the tank by

$$\Delta p_{3(\tau)} = \frac{\Delta p_1 B\left(1 - e^{-\tau/B}\right)}{\left[1 - \left(1 - \frac{\varkappa''\theta''}{\bar{\theta}''}\right) e^{(\varkappa''-1)\tau/\theta''}\right]}, \tag{110}$$

after the cooling chamber by

$$\Delta p_{4(\tau)} = \frac{\Delta p_1 B\left(1 - e^{-\tau/B}\right)\varkappa'\varkappa''}{\left[1 - \left(1 - \frac{\varkappa''\theta''}{\bar{\theta}''}\right) e^{(\varkappa''-1)\tau/\theta''}\right]\left[1 - \left(1 - \frac{\varkappa'\theta'}{\bar{\theta}'}\right) e^{(\varkappa'-1)\tau/\theta'}\right]}, \tag{111}$$

while in the cooling chamber, neglecting the ignition lag ($e^{-st'} \approx 1$)

$$\Delta p_{0(\tau)} = \frac{\Delta p_1 B\left(1 - e^{-\tau/B}\right)\varkappa'\varkappa''\varkappa'''\left(1 - e^{-\tau/\theta'''}\right)}{\left[1 - \left(1 - \frac{\varkappa''\theta''}{\bar{\theta}''}\right) e^{(\varkappa''-1)\tau/\theta''}\right]\left[1 - \left(1 - \frac{\varkappa'\theta'}{\bar{\theta}'}\right) e^{(\varkappa'-1)\tau/\theta'}\right]}. \tag{112}$$

For $\tau = \infty$, the pressure deviation in the combustion chamber approaches the steady value

$$\Delta p_{0(\tau)} = \Delta p_1 B\varkappa'\varkappa''\varkappa'''. \tag{113}$$

If disturbances appear in all supply lines and then propagate into one combustion chamber, the perturbed combustion parameters, reduced to pressure variations, will be expressed by the sum of the individual solutions

$$\alpha_1\Delta p_{01} + \alpha_2\Delta p_{02} + \ldots + \alpha_n\Delta p_{0n} = \sum_1^n \alpha_i \Delta p_i. \tag{114}$$

The results of studies of transients in the supply system using the dynamic differential equations indicate that the various dynamic elements, considered individually, act as inertial elements. Thus in studying their characteristics there is no need to go to equations of second or higher order. The first-order dynamic equations that have been derived are fully adequate for a knowledge of the characteristics of the individual supply-system elements, especially since experimental results confirm the theoretical arguments. Of much greater interest is the form of the final quantity after the disturbance has passed through at least two or three dynamic elements. For a unit disturbance, the solution will be exponential after the disturbance has traversed a single element, but will approach an oscillating form after a second element has been traversed. After the disturbance has passed through two elements, the final quantity will already distinctly have pulsation form, and the solution becomes more distinctly oscillational as the number of elements traversed by the disturbance increases. Since a disturbance of combustion-chamber operation is produced primarily by disturbances in the supply system that have passed through at least two elements, we are led to the conclusion that the combustion chamber has oscillational characteristics. It thus appears that investigations of nonsteady chamber states should be carried out on the basis of at least a second-order differential equation.

6. DETERMINATION OF STABILITY LIMITS

The probability that ranges of unstable operation will appear is less for an engine with constant thrust than for one with variable K. They may appear, however, in certain cases. These include primarily engine startup or a strong disturbance in the supply system. Engine operation under these nonsteady conditions will depend greatly on the values of the engine parameters under steady conditions. Too low combustion-chamber pressure or too low a value for the pressure drop across the injector will render the engine more susceptible to unstable operation. For this reason, presumably, many actual engines use chamber pressures exceeding 25-30 kgf/cm^2, with $\Delta p_{gu} \geq 4$-6 kgf/cm^2. This is most likely due, among other things, to the attempt to avoid eventual appearance of unstable ranges, particularly since where p_0 = 16-18 kgf/cm^2 during starting, the chamber pressure increase does not result in any great increase in specific thrust, but does increase the engine weight disproportionately.

In this section, we propose to determine the limits of operating stability for a rocket motor, specifically a nonisobaric motor. The critical values $\overline{p}_{0kr}$ and $\overline{\Delta p}_{kr}$ can only be determined by means of a dynamic equation describing the nonsteady state for the combustion chamber. Since it has been shown that the chamber is a dynamic oscillating element, a differential equation of at least second order must be used to solve the problem.

Let us now proceed to choose a method for studying the instability ranges. This problem can be solved if we know the roots of the characteristic equation. They can be found by the classical method, using the Encke roots for the lower-order equations, or the Graeffe-Lobachevskiy method for the higher-order equations. This is a very laborious procedure, especially for the higher-order equations. Stability can be evaluated much more rapidly by indirect methods. Considering the specific details of rocket-motor operation, we can divide the existing criteria into two basic groups. In the first group we have the criterion based on the Michailov-Lienhardt determination of roots in a variable connected plane, the criterion developed by the Couchy theorem, and consisting in an examination of the amplitude-phase characteristic, the so-called Nyquist criterion, and the Routh-Hurwitz-Aizerman criterion. In the second we have the Neumark method for D breakdown, the Wysznie-gradzki criterion for region breakdown, and the Evans criterion for the motion of the geometric loci of roots. Using the criteria of the first group, we can only establish whether or not the given engine will operate stably, but we cannot trace the shift in the roots with variation in the parameters. For this reason, these criteria are suitable for analysis of the operating ranges of an existing rocket propulsion system with constant thrust. In designing an engine, we must determine parameters for the chamber (p_0, V_{ks}, D_{ks}/L_{ks}), injector (Δp_{gp}, Δp_{gu}), cooling chamber (W, δ, T_c, p_c), ducts (d, l, w), tanks (p, D), and reduction valve [$p_2 = \psi(p_1)$] for which future performance will be stable. The criteria of the second group meet these requirements, since they lend themselves to investigations using synthesis. Since in our case we are concerned with the determination of the critical parameters, one of the methods from the first group will be adequate.

In the general case, if we have k fuel elements then, together with the oxidizer, every mixture component will have a different ignition lag, in view of the various intrinsic properties of these components. If we take into account the fact that the combustion process takes place at one flame front, however, together with the fact that the variation in properties is small for the classical fuels, all ignition lags can be reduced to one average ignition lag time

$$t' = \sum_{1}^{k'} t/k. \tag{115}$$

If we additionally assume that the supply pressure is the same for all components, we automatically simplify the problem of evaluating the stability of an engine using an n-component propellant to the study of one dynamic differential equation. Equation (36) is just such an equation; it corresponds fully to the model discussed above. The existence of the lag and hence of a back reaction sets up a feedback loop at the chamber and injector, which complicates the construction and analysis of the transfer function. We can use the Nyquist-Mikhailov method, however, after which we need only consider the problem of stability on the basis of the transfer-function operator for the open system that appears when we interrupt the loop. This requires that we expand the exponential function for the delay element into a Taylor series, retaining only the linear terms; this process is not sufficient to determine all of the critical parameters. Let us note, however, that to obtain all these parameters we need only examine the dynamic equation immediately after it is reduced to the characteristic equation, so that the operator transfer function need not be constructed.

We look for a solution in the form

$$p_{0(t)} = Ce^{st}, \quad (p_s - p_0)_{(t-t')} = Ce^{s(t-t')}, \tag{116}$$

for the dynamic startup equation (36), and obtain the characteristic equation

$$1+\theta_1^2 S^2+\theta_2 S-Ne^{-st'} = 0, \tag{117}$$

where $N = 1/kF\sum_{1}^{m} f_i$.

If we now map the left-hand variable connected plane (x, iy) using the function $e^{-st'}$, and rearrange the rest of Eq. (117) for a new system of coordinates, in accordance with the Neumark rule, we will find the stable and unstable regions of engine operation. The intersection of the functions

$$G(\omega) = e^{-i\omega t'}, \tag{118}$$

$$F(\omega) = \frac{\theta_1^2}{N}\omega^2 - i\frac{\theta_2}{N}\omega - \frac{1}{N} \tag{119}$$

defines the stability boundary and, in accordance with the Satche-Nyquist criterion permits construction of the relationships

$$|\sin \omega t'| < \left|\frac{\theta_2}{N}\omega\right|, \tag{120}$$

$$|\cos \omega t'| < \left|\frac{\theta_1^2}{N}\omega^2 - \frac{1}{N}\right|. \tag{121}$$

Using Expressions (120) and (121) and replacing the constants θ_1

and ϑ_2 by the chamber parameters, we obtain the relationships for the lower and upper stability limits for the combustion-chamber pressure with respect to the pressure drop across the injector:

$$p_0 > \frac{2t_0 G R_0 T_0 F_0 \omega^2}{g[R^2\omega^2 + F_0^2 - (\sum_1^m f_i)^2]},$$

$$p_0 < \frac{t_0 G R_0 T_0 \omega^2}{g(F_0 + \sum_1^m f_i \cos\omega t)}. \qquad (122)$$

Analysis of the formula for the upper limit shows that the pressure p_0 can take on values falling considerably outside the range of pressures presently employed for rocket motors. It is only for small pulsations ω and very small Δp_g that the engine can enter the unstable range (Fig. 9). For this reason, there is not much point in studying the upper stability limit considering the pressure drops presently used for injectors and the pulsations occurring.

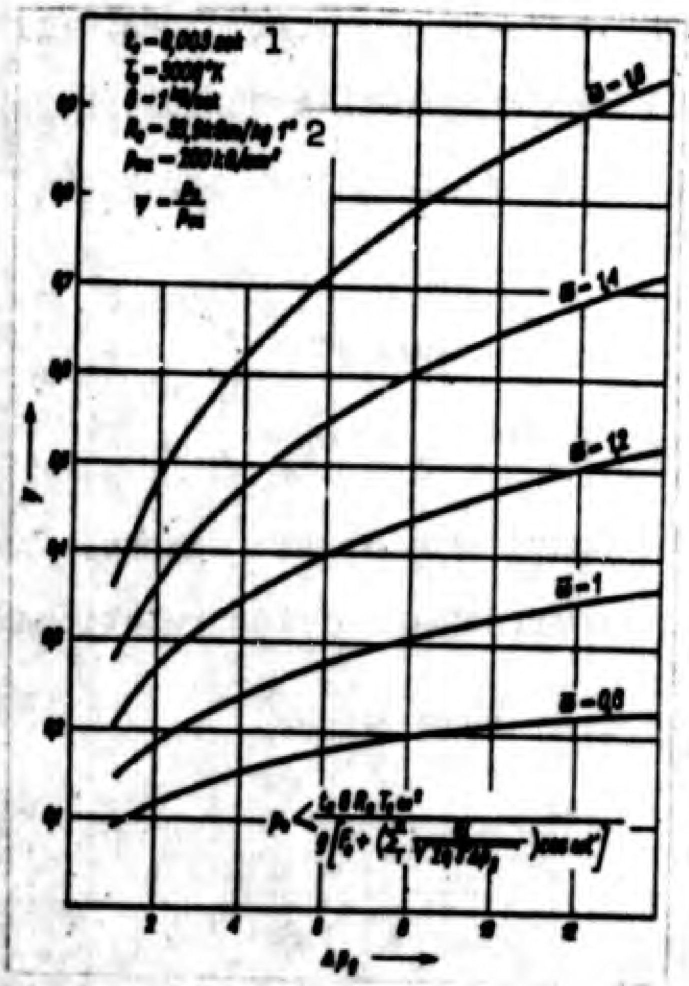

Fig. 9. 1) Sec; 2) kgf-m/kg 1°.

In contrast to $(p_{0kr})_g$, ω has no great effect on the lower stability limit. In view of the small variations in t_0, R_0 and T_0, the type of propellant used also has no great effect on $(\bar{p}_{0kr})$. For a function of the form $p_0 = \varphi(\Delta p_g)$, the coefficient of resistance (R) has the greatest effect on variation in the lower stability limit. Apparently, for low combustion-chamber resistances (Fig. 10), the probability of the engine entering the unstable operating range is high. Theoretical examples indicate, however, that for the Δp_g presently in use and suitably chosen resistances, the lower stability limit is below a pressure of about 15 kgf/cm^2. In this case, the presently employed range of pressures in the combustion chamber could be lowered still more below 20 kgf/cm^2. This would not actually reduce engine efficiency and thrust very much, but would considerably decrease the over-all weight of a rocket-motor stage which is very important in some cases.

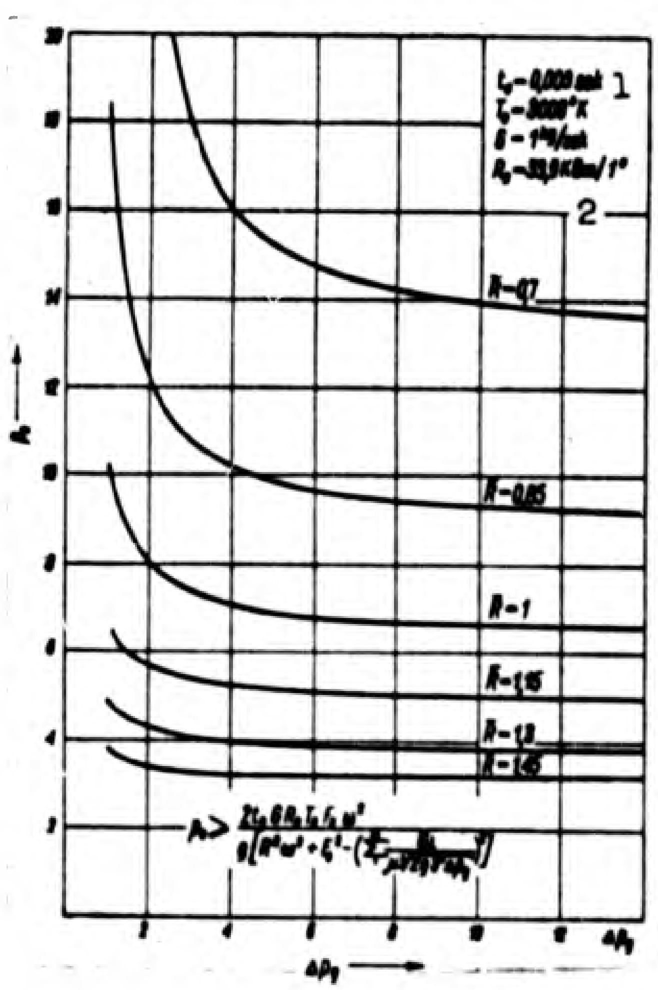

Fig. 10. 1) Sec; 2) kgf-m/1°.

6.1. Pole Singularity of Lower Stability Boundary

For small pulsations and low combustion-chamber damping resistances, the pressure ($\overline{p}_{0kr}$) takes on large values. An increase in the lower limit may also occur where Δp_g decreases sufficiently. In the limiting case, ($\overline{p}_{0kr}$) takes on an infinite value, which means that for a sufficiently small pressure drop across the injector, the engine will perform unstably regardless of the value of the pressure p_0 (Fig. 11). On the basis of Expression (122), we then have

$$(\sqrt{\Delta p_0})_{kr} = \frac{G}{\sqrt{R^2\omega^2 + F_0^2\sqrt{2g\gamma\mu}}} \qquad (123)$$

It should be noted that many scientists such as Crocco, Cheng, Summerfield, and Barrere have already shown experimentally or theoretically that too small a pressure drop Δp_g will always lead to the formation of unstable ranges. It seems that Eq. (123) represents an attempt at analytical definition of absolute instability. For a given propellant (γ_u, γ_p), given chamber parameters (F_0, W, R), and a given injection system (μ), the engine will operate stably if

$$(\sqrt{\Delta p_0})_{kr} < \sqrt{\Delta p_{gr}}. \qquad (124)$$

The analytical definition of Relationship (123) is significant in still another respect. Calculated examples apparently show that ($\overline{\Delta p}_{gkr}$) lies within the range of about 1.5-2.5 kgf/cm^2. Hence we can conclude that it is not really necessary, as with certain engines, to use values $\Delta p_g \approx$ 8-10 kgf/cm^2 that are too high for fear of producing unstable ranges, especially since this leads to an increase in the over-all weight of the motor.

7. COMPARATIVE ANALYSIS

In discussing the basic properties of a nonisobaric rocket motor, it is useful to compare it with the classical engine using a de Laval nozzle. There is no difference whatsoever in the propellant-supply sys-

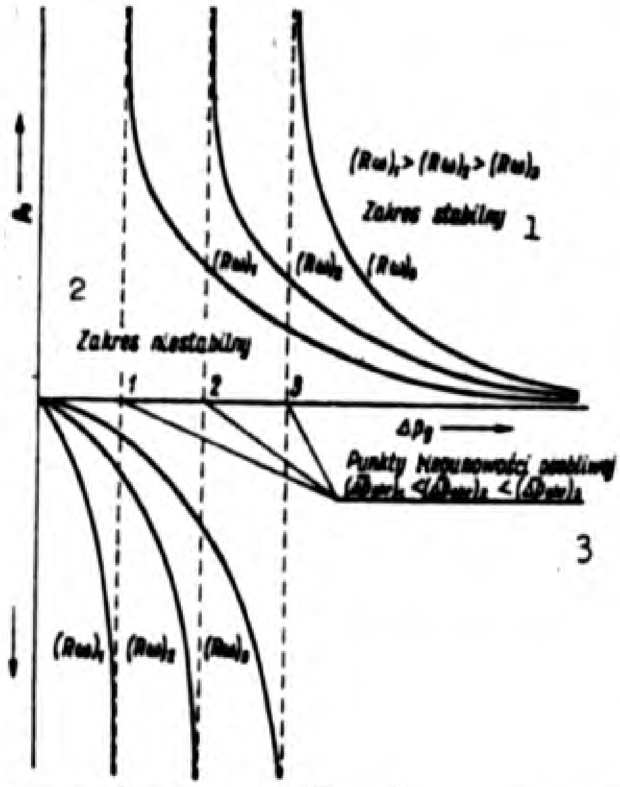

Fig. 11. 1) Stable range; 2) unstable range; 3) singular pole points.

tem, and we can therefore make our comparisons on the basis of the characteristics of the engine itself.

7.1. Engine Parameters

For the identical propellant and identical basic parameters, a nonisobaric engine has smaller α owing to the smaller resistances presented to the flow of gas through the chamber. Where the startup energy for both engines is minimized

$$\int_0^\infty |p_0 - p_{o(\tau)} d\tau|_{is} = \int_0^\infty |p_0 - p_{o(\tau)} d\tau|_{nis} = \min, \qquad (125)$$

for

$$t_{nis} = t_{is} \qquad (126)$$

we have

$$\alpha = \bar{B}\sqrt{p_0}\, D_{ks} L_{ks}, \qquad (127)$$

where

$$\bar{B} = \frac{2\Delta p}{\lambda W_0 \gamma_0 F_0}\sqrt{\frac{g F_0}{t_0 G R_0 T_0}}.$$

Where the lengths of the chamber are identical for both engines, since $D_{ks_{nz}} < D_{ks_{iz}}$, where Condition (125) is satisfied, the combustion chamber pressure should be greater for the nonisobaric engine, or

$$p_{0_{nz}} = p_{0_{iz}} \left(\frac{D_{ks_{iz}}}{D_{ks_{nz}}} \right)^2 \left(\frac{L_{ks_{nz}}}{L_{ks_{iz}}} \right)^2 . \tag{128}$$

In view of the greater heat load, however, the length of the chamber will be greater for the nonisobaric engine and hence the pressure p_0 will not be much greater than the pressure in the isobaric engine.

Using Formulas (61) and (74), we can see that for identical n_0 and α, the values of Δp_{gkr} and $\Delta p_{g(\tau)}$ are smaller for the nonisobaric engine. In order to keep the critical and optimum parameters the same, it is necessary to use a propellant having a shorter ignition lag for the nonisobaric engine. We can thus conclude that the nonisobaric engine is more sensitive than the isobaric engine.

Engine efficiency is very closely connected with the pressure in the combustion chamber. If we assume equal pressure in both engines, together with identical isentropic-expansion exponents, the thermal efficiencies under design conditions will be the same, since

$$\eta_t = 1 - \left(\frac{p_a}{p_0} \right)^{(k-1)/k} . \tag{129}$$

Where startup energy is minimized and equal α_{opt} are used, the thermal efficiency of the nonisobaric engine will be higher in view of the greater chamber pressure. This also applies to the over-all theoretical efficiency. Practically speaking, smaller η_0 can be obtained in view of the more vigorous heat exchange through the wall of the chamber and nozzle.

The nonisobaric engine appears to have a definite advantage with respect to weight. The weight of the entire engine is made up of the sum of the weights of the injector, chamber, and nozzle:

$$Q = Q_g + Q_k + Q_c. \tag{130}$$

The sum $Q_g + Q_k$ may be represented in the form

$$2\frac{\pi D_g^2}{4}\delta_{sr}\gamma_g + \pi D_k L_k \gamma_k \delta_k + \pi D_{chl} L_k \gamma_{chl} \delta_{chl}, \tag{131}$$

where δ_{sr} is the mean thickness of the injector, D_g is the diameter of the injector, γ_g is the specific gravity of the injector-nozzle material, D_k is the mean combustion-chamber diameter, L_k is the length of the combustion chamber, γ_k is the specific gravity of the chamber material, δ_k is the combustion-chamber wall thickness, δ_{chl} is the cooling-chamber diameter, γ_{chl} is the specific gravity of the cooling chamber, and δ_{chl} is the cooling-chamber wall thickness.

On the assumption that

$$D_g \approx D_k \approx D_{chl} = D,$$
$$\gamma_g \approx \gamma_k \approx \gamma_{chl} = \gamma,$$
$$\delta_k \approx \gamma_{chl} \approx \frac{1}{4}\delta_g = \delta = \frac{Dp_{chl}}{2k_r},$$

where k_r is the permissible stress before failure and p_{chl} is the cooling-chamber pressure, Formula (131) will take the form

$$Q_g + Q_k = \frac{\pi\gamma p_{chl} D^2}{k_r}(D + L_k). \tag{132}$$

Remembering that the diameter of the nonisobaric engine D_{nz} will be less by a factor of about 2.5 and the diameter D_{iz} of the isobaric engine and thus assuming

$$D_{nz} = D_{iz}/2{,}5,$$

for $L_{k_{nz}} = L_{k_{iz}} = L_k$, $p_{chl_{nz}} = p_{chl_{iz}}$, $L_{k_{iz}} \approx L_{k_{nz}} = 8D_{nz}$ we obtain

$$\frac{(Q_g + Q_k)_{nz}}{(Q_g + Q_k)_{iz}} = \frac{D_{nz}^2(D_{nz} + L_k)}{D_{iz}^2(D_{iz} + L_k)}. \tag{133}$$

Considering both divergent and convergent-divergent nozzles to have the same weight, and remembering that

$$Q_c \approx 0{,}3(Q_g + Q_k)_{iz},$$

we obtain

$$\boxed{\frac{(Q_1+Q_2+Q_3)_{ni}}{(Q_1+Q_2+Q_3)_{i}} \approx 0{,}335.} \qquad (134)$$

Thus from the standpoint of weight, the nonisobaric engine is to be preferred; it has about one third the weight of the isobaric rocket engine. The advantage is especially pronounced for high-thrust engines. For a unit weight $\underline{q} = 0.03$, an isobaric motor with thrust $K = 10{,}000$ kgf should weight 200 kg, while a nonisobaric motor would weight only 67 kg.

7.2 The Problem of Unsteady Operation and Unsteady Combustion

The problem of unsteady operation is concerned basically with the propellant-supply system alone. Since the supply used for a nonisobaric motor does not differ from that of an isobaric motor, the characteristics of this problem are identical for both types of propulsion systems. Since space-time unsteady combustion depends essentially only on the local variation in mixture composition due to variation in supply pressure, while the latter is determined by the supply-system characteristics, we can conclude that this type of unsteady combustion is just as peculiar to the nonisobaric motor as to the isobaric. It has been shown previously that there exist both forward and back reactions in the nonisobaric engine and hence we can conclude that the isobaric engine is also a dynamic oscillating element with feedback.

7.3. Program for Upper and Lower Stability Limits

In comparing the formulas for the upper stability limit for nonisobaric and isobaric motors, we find that the parameters distinguishing these two engines are the field of the combustion-chamber cross section F_0 and the stay time of the mixture in the chamber. Given the proportions $D_{k_{n}z} = D_{k_{1}z}/2.5$, we have

$$\boxed{F_{0_n} \approx 0{,}16 F_{0_i}.} \qquad (135)$$

It can thus be shown that for the same propellant (t_0, R_0, T_0) and

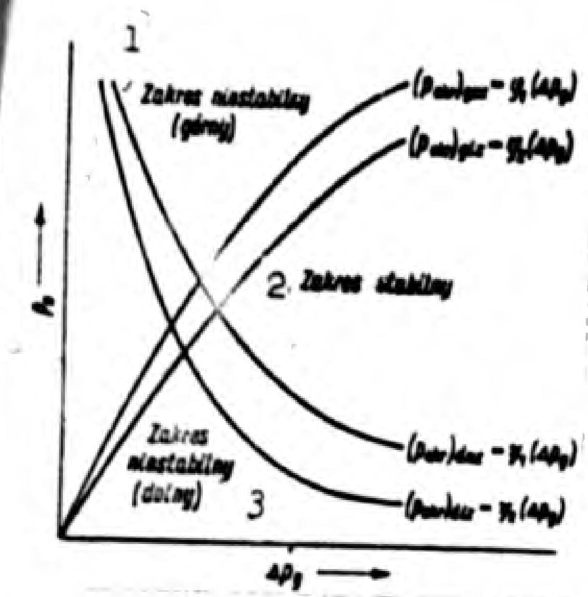

Fig. 12. 1) Unstable range (upper); 2) stable range; 3) unstable range (lower).

the same pulsation ω, the upper stability limit for a nonisobaric motor will move to a chamber pressure value roughly three times that for an engine with a de Laval nozzle. Since the mixture stay time in the engine under consideration is smaller, however, the actual shift in the upper limit will not be so great.

For the lower limit, the two engines compared vary in the magnitude of the field (F_0), the chamber loss coefficient (R), and, eventually, the stay time (t_0). For identical propellants, pulsations, and resistances, the lower limit moves toward higher combustion-chamber pressures for the nonisobaric engine. The same conclusion applies to the effect of R. Only a briefer t_0 for the nonisobaric engine can reduce the upward shift of the lower limit.

This analysis leads to the conclusion that the stable operating range of a nonisobaric engine moves toward higher combustion-chamber pressures (Fig. 12).

Since the lower limit is displaced more than the upper limit for both of the engines compared, the field of the stable operating range is greater, however, for the isobaric engine and the nonisobaric engine is more sensitive in this respect.

7.4. Prospects for the Nonisobaric Motor

In the isobaric motor, the chamber pressure is greater than p_0 owing to parameter optimization and the higher lower limit of stability. It is true that this leads to an improvement in efficiency, but at the same time it impairs the weight characteristics of the supply system. On the other hand, a nonisobaric motor is much lighter than an isobaric motor. This weight difference becomes particularly apparent in high-thrust propulsion systems. Hence we must conclude that nonisobaric rocket motors deserve attention, particularly for small or very large units. It is true that for low-K engines we gain little with respect to engine weight, but even a small increase in the propellant-supply system weight contributes to better efficiency. In large-K engines, even though the weight of the supply installation is only slightly greater than for an isobaric motor, we can gain considerably owing to the decreased weight of the motor itself. Since combustion efficiency is greater for large chambers, we conclude that nonisobaric motors are promising subjects for development, particularly in very large units.

8. CONCLUSIONS

The critical and optimum parameters defined can be used to introduce certain corrections into the existing methods of designing liquid rocket motors. Following a preliminary determination of the thermal and geometric parameters of the motor for a given propellant (γ, T_0, t_0) using the earlier methods, $(\Delta p_{gkr})_u$, p_{0opt}, and $\Delta p_{g(\tau)}$ should be determined for the initial operating period. If the critical value found for the pressure drop across the injector is considerably smaller than that assumed, the computation should be repeated. The value of the combustion-chamber pressure should also be suitably corrected so as to bring it as close as possible to the optimum value. The upper and lower stability limits should be determined next, and a suitable safety factor allowed. Following the calculations for the startup period, it is advisable to check the critical value for the pressure drop across the injector $(\Delta p_{gkr})_{(\tau = 0)}$ and to compare this value with the static value $(p_z - p_0)$. If there is no pronounced excess

$$(\Delta p_{gkr})_{(\tau=0)} > (p_z - p_0),$$

it is necessary to control the propellant flow-rate during the first phase of engine operation, in accordance with the function

$$(p_s - p_0) = (p-1)e^{-\psi\varphi_1} + \Delta p_{gu}.$$

It is quite possible that in some cases determination of the critical and optimum parameters will require more repetition of the calculations than is required by the classical method previously used. Difficulties may also be encountered in determining the pulsation (ω) and the loss coefficient for the combustion chamber (R). Still, the introduction of these corrections offers certain advantages, the most important of which are:

1. The results of sample calculations show that both $(\Delta p_{gkr})_u$ and p_{0opt} are lower in value than for some actual rocket motors. For certain combinations of parameters, it may turn out that the introduction of these corrections can reduce the over-all motor weight with only a slight reduction in thrust (Fig. 13).

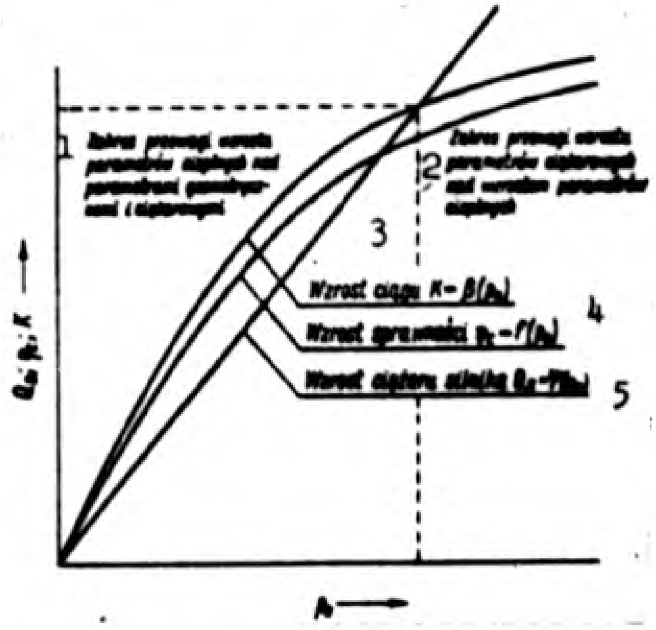

Fig. 13. 1) Range in which thermal parameters increase more rapidly than geometrical and weight parameters; 2) range in which weight parameters increase more rapidly than thermal parameters; 3) increase in thrust $K = \beta(p_0)$; 4) increase in efficiency $\eta_c = f(p_0)$; 5) increase in engine weight $Q_s = \psi(p_0)$.

2. Consideration of the nonsteady-state results gives the existing method a dynamic aspect. Certain singular characteristics thus appear during the design stage of engine development rather than in the later

experimental stage.

3. The proposed corrections permit analytical determination of startup parameters; this is the most complicated period of engine op ation. Determination of $(\Delta p_{gkr})_{(\tau = 0)}$ can alert the designer to ran ngerous to the engine in the design stage, while determination of $(p_z - p_0) = \psi(\tau)$ can help him ensure smooth startup. Under certain c ditions, such analytical procedures may ultimately reduce the experi mental testing required.*

Military Technical Academy

Received November 1962

Manu-script Page No.	[Footnote]
50	I wish to thank Professor Dr. R. Szymanik for direction and valuable guidance received in the course of this study. I a so consider it my pleasant duty to thank Prof. Dr. h.c. B. Stefanowski, as well as Docent Dr. B. Staniszewski and Doce Dr. S. Wojcicki for permission to present this paper at the Doctors' Seminar at the Department of Technical Engineering of the Warsaw Polytechnical Institute, and for their valuab comments.

er-
ges
on-
-
l-
nt
le

REFERENCES

1. M. Barrere, A. Jamotte, B. Traeijs de Veubeke and J. Vandekerckove: La Probulsion Par Fusees. Dunod 1957.
2. E.A. Bonney, M.I. Zucrowe and W. Besserer: Aerodynamic Propulsion Structures and Design Practice. D. Van Nostrand Company, Inc. New York, London,1956.
3. N. Crocco and S. Chang: Theory of Combustion Instability in Liquid Propellant Rocket Motors. Butterworth Scientific Publications, 1956.
4. H. Margenau and G.M. Murphy: Matematyka w fizyce i chemii. [Mathematics in Physics and Chemistry], PWN, Warsaw, 1956.
5. D. Shin and I. Pai: Fluid Dynamics of Jets. D. Van Nostrand Company, Inc.,New York, 1954.
6. B. Stefanowski and B. Staniszewski: Termodynamika techniczna. [Engineering Thermodynamics], Warsaw, 1959.
7. M.W. Thring, O. Lutz, J. Fabri and H. Lefebvre: Combustion and Propulsion, Third Agard Colloqium. Pergamon Press, 1958.

DISTRIBUTION LIST

DEPARTMENT OF DEFENSE	Nr. Copies	MAJOR AIR COMMANDS	Nr. Copies
		DDC	20
		AFSC	
		SCFDD	1
		TDBTL	5
		TDBDP	2
		TDGS	1
HEADQUARTERS USAF		AEDC (AEY)	1
		AFFTC (FTF)	1
AFNINDE	1	AFWL (WLF)	1
ARL (ARB)	1	ASD (ASFA)	2
		BSD (BSF)	1
		ESD (ESY)	1
		SSD (SSF)	2

OTHER AGENCIES

CIA	5
NSA	6
DIA	4
AID	2
OTS	2
AEC	2
PWS	1
NASA (ATSS-T)	1
ARMY (FSTC)	3
NAVY	3
NAFEC	1
PGE	12
AFCRL (CRXLR)	1
FAA (SS-10)	1
SPECTRUM	1